Motion Segmentation in the Presence of Outlying, Incomplete, or Corrupted Trajectories

Journal:	*Transactions on Pattern Analysis and Machine Intelligence*
Manuscript ID:	draft
Manuscript Type:	Regular
Keywords:	I.4.8.d Motion < I.4.8 Scene Analysis < I.4 Image Processing and Computer Vision < I Computing Methodologies, I.5.3 Clustering < I.5 Pattern Recognition < I Computing Methodologies

Motion Segmentation in the Presence of Outlying, Incomplete, or Corrupted Trajectories

Shankar Rao, *Student Member, IEEE,* Roberto Tron, *Student Member, IEEE,* René Vidal, *Member, IEEE,* and Yi Ma, *Senior Member, IEEE*

Abstract

In this paper, we study the problem of segmenting tracked feature point trajectories of multiple moving objects in an image sequence. Using the affine camera model, this problem can be cast as the problem of segmenting samples drawn from multiple linear subspaces. In practice, due to limitations of the tracker, occlusions, and the presence of nonrigid objects in the scene, the obtained motion trajectories may contain grossly mistracked features, missing entries, or corrupted entries. In this paper, we develop a robust subspace separation scheme that deals with these practical issues in a unified mathematical framework. Our methods draw strong connections between lossy compression, rank minimization, and sparse representation. We test our methods extensively on the Hopkins155 motion segmentation database and other motion sequences with outliers and missing data. We compare the performance of our methods to state-of-the-art motion segmentation methods based on expectation-maximization and spectral clustering. For data without outliers or missing information, the results of our methods are on par with the state-of-the-art results, and in many cases exceed them. In addition, our methods give surprisingly good performance in the presence of the three types of pathological trajectories mentioned above. All code and results are publicly available at `http://perception.csl.uiuc.edu/coding/motion/`.

Index Terms

Motion Segmentation, Subspace Separation, Lossy Compression, Incomplete Data, Error Correction, Sparse Representation, Matrix Rank Minimization.

I. Introduction

A fundamental problem in computer vision is to infer structures and movements of 3D objects from a video sequence. While classical multiple-view geometry typically deals with the situation where the scene is static, recently there has been growing interest in the analysis of dynamic scenes. Such scenes often contain multiple motions, as there could be multiple objects moving independently in a scene, in addition to the motion of the camera. Thus an important initial step in the analysis of video sequences is the *motion segmentation* problem. That is, given a set of feature points that are tracked through a sequence of video frames, one seeks to cluster the trajectories of those points according to the different motions these trajectories belong to.

In the literature, many different camera models have been proposed and studied, such as orthographic, paraperspective, affine, and perspective. Among these the affine camera model

(which includes orthographic and paraperspective) is arguably the most popular, due largely to its generality and simplicity. Thus, in this paper, we assume the affine camera model, and show how to develop a more robust solution to the motion segmentation problem.

A. Basic Formulation of Motion Segmentation

Under the affine camera model a feature point in 3-D space $(X, Y, Z) \in \mathbb{R}^3$ is related to its projection on the image plane $(x, y) \in \mathbb{R}^2$ by

$$\begin{bmatrix} x \\ y \end{bmatrix} = \underbrace{K \begin{bmatrix} 1\,0\,0\,0 \\ 0\,1\,0\,0 \\ 0\,0\,0\,1 \end{bmatrix} \begin{bmatrix} R & \boldsymbol{t} \\ \mathbf{0}^T & 1 \end{bmatrix}}_{A \in \mathbb{R}^{2\times 4}} \begin{bmatrix} X \\ Y \\ Z \\ 1 \end{bmatrix}, \tag{1}$$

where A is the *affine motion matrix*, parameterized by the camera calibration matrix $K \in \mathbb{R}^{2\times 3}$ and the relative orientation of the image plane with respect to the world coordinates $(R, \boldsymbol{t}) \in SE(3)$.

Suppose we are given trajectories of P tracked feature points of a rigid object $\{(x_{fp}, y_{fp})\}_{f=1\ldots F}^{p=1\ldots P}$ from F 2-D image frames of a rigidly moving camera. The linear constraints in (1) can be combined for multiple points across multiple frames so that the tracked feature points are related to their 3-D coordinates $\{(X_p, Y_p, Z_p)\}_{p=1}^{P}$ by the matrix equation:

$$\underbrace{\begin{bmatrix} x_{11} & x_{12} & \cdots & x_{1P} \\ y_{11} & y_{12} & \cdots & y_{2P} \\ \vdots & \vdots & \ddots & \vdots \\ x_{F1} & x_{F2} & \cdots & x_{FP} \\ y_{F1} & y_{F2} & \cdots & y_{FP} \end{bmatrix}}_{\mathtt{Y} \in \mathbb{R}^{2F\times P}} = \underbrace{\begin{bmatrix} A_1 \\ \vdots \\ A_F \end{bmatrix}}_{\mathtt{A} \in \mathbb{R}^{2F\times 4}} \underbrace{\begin{bmatrix} X_1 & \cdots & X_P \\ Y_1 & \cdots & Y_P \\ Z_1 & \cdots & Z_P \\ 1 & \cdots & 1 \end{bmatrix}}_{\mathtt{X} \in \mathbb{R}^{4\times P}},$$

$$\mathtt{Y} = \mathtt{A}\mathtt{X} \tag{2}$$

where A_f is the affine motion matrix at frame f. From this formulation we see that

$$\text{rank}(\mathtt{Y}) = \text{rank}(\mathtt{A}\mathtt{X}) \leq \min(\text{rank}(\mathtt{A}), \text{rank}(\mathtt{X})) \leq 4. \tag{3}$$

Thus the affine camera model postulates that trajectories of feature points from a single rigid motion will all lie in a linear subspace of $\mathbb{R}^{2F}$ of dimension at most four.

A dynamic scene can contain multiple moving objects, in which case the affine camera model for a single rigid motion cannot be directly applied. Now let us assume that the given P trajectories correspond to N moving objects. In this case, the set of all trajectories will lie in a *union of N linear subspaces* in $\mathbb{R}^{2F}$ (see, for instance, [27] for details), but we do not know which trajectories belongs to which subspace. Thus, the problem of assigning each trajectory to its corresponding motion reduces to the problem of segmenting data drawn from multiple subspaces, which we refer to as *subspace separation*.

Problem 1: **(Motion Segmentation via Subspace Separation)** Given a set of trajectories of P feature points $\mathtt{Y} = [\boldsymbol{y}_1, \boldsymbol{y}_2, \ldots, \boldsymbol{y}_P] \in \mathbb{R}^{2F \times P}$ from N rigidly moving objects in a dynamic scene, find a permutation Γ of the columns of the data matrix $\mathtt{Y}$:

$$\mathtt{Y}\Gamma = [\mathtt{Y}_1, \mathtt{Y}_2, \ldots, \mathtt{Y}_N], \tag{4}$$

such that the columns of each submatrix $\mathtt{Y}_n$, $n = 1, \ldots, N$, are trajectories of a single motion.

B. Related Work on Motion Segmentation

In the literature, there are many approaches to motion segmentation, that can roughly be grouped into three categories: factorization-based, algebraic, and statistical.

Factorization-based approaches [5], [12], [16], [17] attempt to directly factor $\mathtt{Y}$ according to (4). To make such approaches tractable, the motions must be independent of one another, i.e. the motion subspaces intersect only at the origin. However, for most dynamic scenes with a moving camera or containing articulated objects, the motions are at least partially dependent on each other. This has motivated the development of algorithms designed to deal with dependent motions.

Algebraic methods, such as Generalized Principal Component Analysis (GPCA) [26], are designed as generic subspace separation algorithms that do not place any restriction on the relative orientations of the motion subspaces. For instance, they allow the subspaces to intersect into lower-dimensional subspaces, and hence they can deal with partially dependent motions. In principle, algebraic methods such as GPCA can be extended to deal with missing data [27] and outliers [32]. However, its complexity grows *exponentially* with respect to both the dimension of the ambient space and the number of motions in the scene, and so is not scalable in practice.

The statistical methods come in many flavors. Many formulate motion segmentation as a statistical clustering problem that is tackled with Expectation-Maximization (EM) or variations of it [23], [18], [14]. As such, they are iterative methods that require good initialization, and can potentially get stuck in suboptimal local minima. Other statistical methods use local information around each trajectory to create a pairwise similarity matrix that can then be segmented using *spectral clustering* techniques [33], [31], [10].

C. Robustness Issue

Many of the above approaches assume that all trajectories are good, with perhaps a moderate amount of noise. However, real motion data acquired by a tracker can be much more complicated:

1) A trajectory may correspond to certain nonrigid or random motions that do not obey the affine camera model (an *outlying trajectory*).
2) Some of the features may be missing in some frames, causing a trajectory to have some missing entries (an *incomplete trajectory*).
3) Even worse, some feature points may be mistracked (with the tracker unaware), causing a trajectory to have some entries with gross errors (a *corrupted trajectory*).

While some of the methods can be modified to be robust to *one* of such problems [14], [10], [32], [31], [27], to our knowledge there is no motion segmentation algorithm that can elegantly deal with all of these problems in a unified fashion.

D. Our Approach

In order to uniformly and effectively deal with clustering and robustness issues, we rely on Occam's Razor: *All other things being equal, the simplest solution is the best*. This means that when choosing among multiple viable segmentations for motion data, one should pick the segmentation that most simply explains the data. There are many empirical metrics that can be used to express the simplicity of data. One of such measures is the *coding length*, which is the minimal number of bits needed to represent data. The coding length has been used effectively for data compression and model selection [1] as well as for segmentation [20]. In recent years, there has been increasing interest in findings representations for data that are *sparse*, i.e., having few nonzero entries. This interest has been mainly fueled by the discovery that, when the sparsity is high enough, such representations can be efficiently computed using convex optimization [8],

[4]. The sparse structure of data has also been shown to be highly robust and can be used to deal with incomplete and corrupted data [3].

In this paper, we propose a new motion segmentation scheme that draws heavily from the principles of both *data compression* and *sparse representation*. We show that the notion of coding length and sparsity are highly related, and by properly exploiting them, we are able to make motion segmentation robust to all three types of pathological trajectories listed above. In particular, we adapt the lossy compression-based agglomerative clustering algorithm from [20], referred to as *Agglomerative Lossy Compression (ALC)*, to the problem of motion segmentation. The algorithm is noniterative, and requires only a single parameter. We will show how it can be naturally adapted to deal with outliers in our context. We supplement ALC with techniques from sparse representation, allowing our method to handle incomplete and corrupted trajectories even before the segmentation is obtained. To our knowledge, our paper is the first to apply sparse representation to the problem of motion segmentation.

Organization of this paper. We first review our agglomerative algorithm (§II-A), then show how we apply the derived algorithm to motion segmentation (§II-B), and test the effectiveness of the algorithm on the publicly available Hopkins155 motion segmentation database (§II-C). We show that the new algorithm naturally handles outlying trajectories (§III-A), and can be extended to repair incomplete (§III-B) or corrupted trajectories (§III-C). Note our distinction between incomplete and corrupted trajectories: for incomplete trajectories, we know in which frames the features are missing; for corrupted ones, we do not have that knowledge. Our methods use the affine camera model assumption, so we make comparisons with similar methods, but not with perspective camera-based methods[1]. As most extant methods for motion segmentation assume that the number of motions is known, for fair comparison, we also assume the group count is given.

II. Agglomerative Lossy Compression (ALC)

In this section, we describe the subspace separation method that we use for motion segmentation. §II-A reviews the principles of matrix rank minimization, data compression, and sparse

[1]Please refer to [22] for work on robust motion segmentation with a perspective camera model.

representation behind ALC. §II-B shows how ALC can be applied to the motion segmentation problem when the motion trajectories are complete and contain no outliers.

A. Matrix Rank Minimization and Lossy Data Compression

According to the problem formulation (4), to a large extent, the goal of subspace separation is to find a partition of the data matrix $\mathtt{Y}$ into submatrices $\{\mathtt{Y}_n\}_{n=1}^N$ such that each $\mathtt{Y}_n$ spans a subspace of the lowest possible dimension. In other words, each $\mathtt{Y}_n$ as a matrix is maximally rank deficient. *Matrix rank minimization* (MRM) is itself a very challenging problem. The rank function is neither smooth nor convex, and it is notoriously difficult to minimize directly. Finding a matrix $\mathtt{M}$ that is maximally rank deficient among a convex set of matrices is known to be NP-Hard [25]. Also, the rank function is highly unstable in the presence of noise. Recent progress in compressed sensing has led to some groundbreaking work in rank minimization. In particular, it has been shown that when the matrix rank is low enough, minimizing the matrix rank over a convex domain is equivalent to minimizing the matrix nuclear norm[2] $\|\mathtt{M}\|_*$, which can be solved efficiently by semi-definite programming [21].

However, here we are not minimizing $\text{rank}(\mathtt{Y}_n)$ over a convex set. The number of segmentations of the data matrix $\mathtt{Y}$ into $\{\mathtt{Y}_n\}_{n=1}^N$ is combinatorial and this makes the space of all segmentations of $\mathtt{Y}$ a very complicated domain. Thus, technically subspace separation *cannot* be reduced to an instance of MRM over a convex domain. This forces us to seek other alternative surrogates for matrix rank. For a positive semidefinite matrix $\mathtt{M} \in \mathbb{R}^{D\times D}$, one can deal with both instability and computational intractability of matrix rank by minimizing the following function instead:

$$J(\mathtt{M}, \delta) \doteq \log_2 \det\left(\mathtt{I} + \tfrac{1}{\delta}\mathtt{M}\right), \tag{5}$$

where $\delta > 0$ is a small regularization parameter [11]. It is easy to see that the function J is approximately the sum of the logarithm of the singular values (up to a scale). So unlike the nuclear norm which is convex, the function J is no longer convex, though it is a smooth surrogate. Nevertheless, $J(\mathtt{M}, \delta)$ has the same global minimum as $\text{rank}(\mathtt{M})$, as shown in Figure 1 (for each singular value).

[2]The nuclear norm of a matrix $\mathtt{M}$ is the sum of all its singular values $\sum_i \sigma_i$.

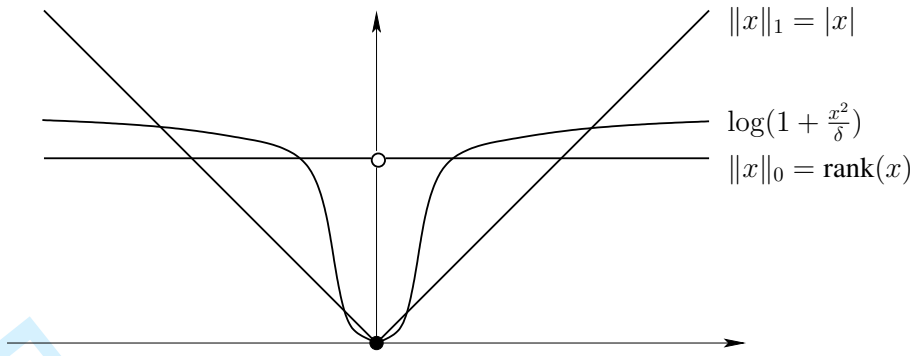

Fig. 1. Comparison of $J(x, \delta)$, $\text{rank}(x) = \|x\|_0$, and the nuclear norm (1-norm) $\|x\|_1 = |x|$ in one dimension.

After a slight modification to (5), we can see a clear connection between the above surrogate and the principle of (lossy) *minimum description length* (MDL) [20]. Given data $\mathtt{Y}_n \in \mathbb{R}^{D \times P_n}$ drawn from a linear subspace, the number of bits needed to code the data $\mathtt{Y}_n$ up to distortion ε^2 [20][3] is given by

$$L(\mathtt{Y}_n, \varepsilon) \doteq \frac{D + P_n}{2} J\left(\frac{1}{P_n}\mathtt{Y}_n\mathtt{Y}_n^T, \frac{\varepsilon^2}{D}\right) = \frac{D + P_n}{2} \log_2 \det\left(\mathtt{I} + \frac{D}{P_n\varepsilon^2}\mathtt{Y}_n\mathtt{Y}_n^T\right). \tag{6}$$

This function is still a smooth surrogate for $\text{rank}(\mathtt{Y}_n)$, as it is obtained by scaling $J(\mathtt{M}, \delta)$ by a constant term, with $\mathtt{M} = \frac{1}{P_n}\mathtt{Y}_n\mathtt{Y}_n^T$ and $\delta = \frac{\varepsilon^2}{D}$.

Now suppose the data matrix $\mathtt{Y} \in \mathbb{R}^{D \times P}$, can be partitioned into disjoint subsets $\mathtt{Y} = [\mathtt{Y}_1 \ldots \mathtt{Y}_N]$ of corresponding sizes $P_1 + \cdots + P_N = P$. If we encode each subset separately, the total number of bits required is

$$L^s(\{\mathtt{Y}_1, \ldots, \mathtt{Y}_N\}, \varepsilon) \doteq \sum_{n=1}^{N} L(\mathtt{Y}_n, \varepsilon) - P_n \log_2 \frac{P_n}{P}. \tag{7}$$

The second term in this equation counts the number of bits needed to represent the membership of the P vectors in the N subsets (e.g., by Huffman coding). In [20], Ma et al. posit that the optimal segmentation of the data minimizes the number of bits needed to encode the segmented data up to distortion ε^2. It is worth noticing that, once the distorsion parameter ε is fixed, the number of groups in the segmentation is automatically determined. This completely avoids the

[3]It can be shown that as $\varepsilon \to 0$, (6) converges to the optimal rate distortion for a Gaussian source, and it is also an upper bound for the coding length of subspace-like data.

necessity of additional model-selection criterion usually required with traditional segmentation methods.

The issue now is that finding a global minimum of (7) is a combinatorial problem. Nevertheless, an agglomerative algorithm, proposed in [20], has been shown to be very effective for minimizing (7). Algorithm 1, listed below, initially treats each sample as its own group, iteratively merging pairs of groups so that the resulting coding length is maximally reduced at each iteration. The algorithm terminates when it can no longer reduce the coding length. We refer to Algorithm 1 as *Agglomerative Lossy Compression* (ALC). See [20] for more details.

Algorithm 1 (Agglomerative Lossy Compression).

Input: $\mathtt{Y} = [\boldsymbol{y}_1, \boldsymbol{y}_2, \ldots, \boldsymbol{y}_P] \in \mathbb{R}^{D \times P}, \varepsilon \in \mathbb{R}$
Let $\mathcal{S} = \{\{\boldsymbol{y}_1\}, \ldots, \{\boldsymbol{y}_P\}\}$
`done` := `false`
while not `done` **do**
  $\{\mathtt{Y}_i^*, \mathtt{Y}_j^*\} := \underset{\{\mathtt{Y}_i, \mathtt{Y}_j\} \in \mathcal{S}}{\operatorname{argmin}} \; L^s(\{[\mathtt{Y}_i \; \mathtt{Y}_j]\}, \varepsilon) - L^s(\{\mathtt{Y}_i, \mathtt{Y}_j\}, \varepsilon)$
  if $L^s(\{[\mathtt{Y}_i^* \; \mathtt{Y}_j^*]\}, \varepsilon) - L^s(\{\mathtt{Y}_i^*, \mathtt{Y}_j^*\}, \varepsilon) \geq 0$ **then**
    `done` := `true`
  else
    $\mathcal{S} := \big(\mathcal{S} \setminus \{\mathtt{Y}_i^*, \mathtt{Y}_j^*\}\big) \cup \{[\mathtt{Y}_i^* \; \mathtt{Y}_j^*]\}$
  end if
end while
output: $\mathcal{S}$

B. Applying ALC to Motion Segmentation

ALC can be immediately applied to the motion segmentation problem in the case of complete trajectories with no outliers. However, since the $2F$-dimensional trajectories of N rigid-body motions live in a subspace of dimension at most $4N$, most existing motion segmentation algorithms precede clustering by a dimensionality reduction step. Therefore, the performance of ALC will be affected by the choice of the dimension $d \leq 2F$ of the low-dimensional subspace onto which the original data is projected onto. Another parameter that will affect the performance of ALC

is the variance of the noise ε. In this subsection, we describe some methods for choosing these parameters in the context of motion segmentation. We also discuss the computational complexity of the method, and show how it can be improved.

Choosing ε. In principle, ε could be determined in some heuristic fashion from the statistics of the data, see e.g., [17]. However, notice that the variance of the noise ε is directly related to the number of motions N: the smaller ε the larger N and viceversa. Since most extant motion segmentation algorithms require the number of motions as a parameter, in order to make a fair comparison with other methods, we assume that the number of motions is given, and use it to determine ε. Figure 2 shows an example motion sequence. We run ALC on this sequence for several choices of ε. On the right we plot the misclassification rate and estimated group count as a function of ε. We see that the correct segmentation is stable over a fairly large interval. Using this observation, we developed the following voting scheme:

1) For a given motion sequence, run the algorithm multiple times over a number of choices of ε.[4]
2) Discard any ε that does not give rise to a segmentation with the correct number of groups.[5]
3) With the remaining choices of ε, find all the distinct segmentations that are produced.
4) Choose the ε that minimizes the coding length for the most segmentations, relative to the other choices of ε.

This scheme is quite simple, and by no means optimal, but as our experiments show, it works very well in practice.

Choosing the dimensionality of projection. Dimensionality reduction can improve the computational tractability of subspace separation without adversely affecting the quality of the segmentation. This is because, with probability one, projection onto an arbitrary d-dimensional subspace preserves the multi-subspace structure of data lying on subspaces with dimensionality strictly less than d. Thus, for segmenting affine motions, [27] suggests projecting the trajectories onto a 5-dimensional subspace. However, for more complicated scenes (e.g. scenes with articulated or nonrigid motion), five dimensions may not be sufficient.

[4]Our experiments use 101 steps of ε in the interval $[10^{-5}, 10^{3}]$.

[5]If none of the choices of ε produce the right number of groups, we select the ε that minimizes the "penalized" coding length proposed in [20].

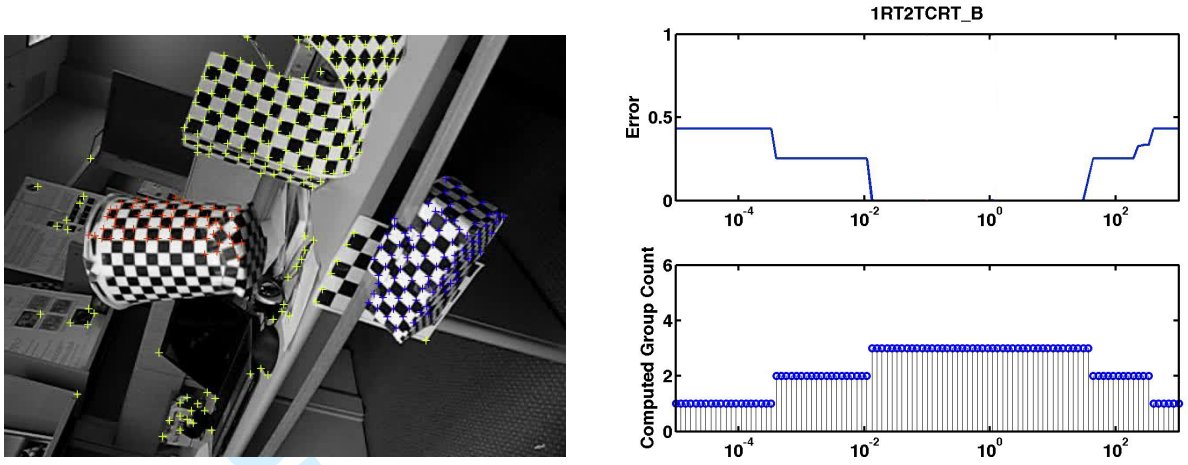

Fig. 2. Left: The "1RT2TCRT_B" sequence from the Hopkins155 database. Right: The misclassification rate and estimated group count as a function of ε.

The running time ALC is polynomial w.r.t. dimension, so, in principle, we could leave our data in a relatively high-dimensional space. However, recall that ALC applies a greedy approach to make minimization of (7) computationally feasible. Due to its greedy nature, ALC can obtain a segmentation that does not globally minimize the coding length. In fact, precise theoretical conditions for ALC to converge to the minimum coding length segmentation are not yet known. Ma et al. demonstrated empirically that, for data in high-dimensional spaces, suboptimal segmentations can be found if the samples do not adequately cover each subspace [20]. Thus, dimensionality reduction can potentially improve the results of ALC by making the subspaces more dense with samples.

A balance needs to be struck between expressiveness and sample density. One choice, recently proposed in the sparse representation community [9], is the *sparsity-preserving* dimension d_{sp}:

$$d_{\text{sp}} = \min d \quad \text{subject to} \quad d \geq 2k \log(D/d), \tag{8}$$

where D is the dimension of the ambient space and k is the true low dimension of the data. It has been shown, that, asymptotically, as $D \to \infty$, this d is the smallest projection dimension such that the low-dimensional multi-subspace structure of the data is preserved with high probability under a *random* projection. For our problem, using the affine camera model, the dimension of the motion subspaces is at most 4, so we can assume that $k = 4$ and obtain a conservative estimate for the dimensionality of projection d. As our experimental results will show, this choice works

well in practice.

In our experiments, we test ALC with projection dimensions $d = 5$ (as suggested in [27]), and the sparsity-preserving d stated above. We refer to the two versions of the algorithm as ALC_5 and ALC_{SP}, respectively.

Algorithmic improvements to ALC. As discussed in [20], the computational complexity of a straightforward implementation of ALC is

$$O(P^3 + P^2 D^3). \tag{9}$$

The first term in (9) corresponds to, for each of $O(P)$ iterations, searching a table of size $O(P) \times O(P)$ for the pair of groups that, when merged, maximally decrease the overall coding length. The second term in (9) corresponds to, for each of $O(P)$ iterations, the cost of updating $O(P)$ entries in the table via an $O(D^3)$ log-determinant computation. In practice, the running time of ALC is dominated by this second term. We have observed empirically that, the vast majority of the time, one of the two groups to be merged contains only one sample. In this case, the log-determinant can be computed via a rank-1 update to the Cholesky factorization of a $D \times D$ matrix [29]. By doing so, the computational complexity of ALC becomes

$$O(P^3 + P^2 D^2 + P D^3), \tag{10}$$

allowing the speed of ALC to scale more gracefully with the dimensionality of the data. We quantitatively demonstrate this decrease in the running time of ALC in the next section.

C. Results on the Hopkins155 Database

We now test the efficacy of ALC for motion segmentation, by applying the algorithm to the Hopkins155 database [24]. The Hopkins155 database consists of 155 motion sequences that can be categorized as checkerboard, traffic, or articulated. The motion sequences were obtained using an automatic tracker, and errors in tracking were manually corrected for each sequence. Thus in this experiment, there is no attempt to deal with incomplete or corrupted trajectories. See [24] for more details on the Hopkins155 database.

We run ALC_5 and ALC_{SP} on the checkerboard, traffic, and articulated sequences using the voting scheme described earlier to determine ε. For each category of sequences, we compute the average and median misclassification rates, and the average computation times. We list these

(a) 2-motion sequences

Checkerboard	MSL	LSA	ALC_5	ALC_{sp}
Average	4.46%	2.57%	2.56%	**1.49%**
Median	0.00%	0.27%	0.00%	0.27%
Traffic	MSL	LSA	ALC_5	ALC_{sp}
Average	2.23%	5.43%	2.83%	**1.75%**
Median	0.00%	1.48%	0.30%	1.51%
Articulated	MSL	LSA	ALC_5	ALC_{sp}
Average	7.23%	**4.10%**	6.90%	10.70%
Median	0.00%	1.22%	0.89%	0.95%
All Sequences	MSL	LSA	ALC_5	ALC_{sp}
Average	4.14%	3.45%	3.03%	**2.40%**
Median	0.00%	0.59%	0.00%	0.43%

(b) 3-motion sequences

Checkerboard	MSL	LSA	ALC_5	ALC_{sp}
Average	10.38%	5.80%	6.78%	**5.00%**
Median	4.61%	1.77%	0.92%	0.66%
Traffic	MSL	LSA	ALC_5	ALC_{sp}
Average	**1.80%**	25.07%	4.01%	8.86%
Median	0.00%	23.79%	1.35%	0.51%
Articulated	MSL	LSA	ALC_5	ALC_{sp}
Average	**2.71%**	7.25%	7.25%	21.08%
Median	2.71%	7.25%	7.25%	21.08%
All Sequences	MSL	LSA	ALC_5	ALC_{sp}
Average	8.23%	9.73%	**6.26%**	6.69%
Median	1.76%	2.33%	1.02%	0.67%

TABLE I

MISCLASSIFICATION RATES [%] FOR SEQUENCES OF TWO AND THREE MOTIONS IN THE HOPKINS155 DATABASE.

results in Tables I and II along with the reported results for Multi-Stage Learning (MSL) [18] and Local Subspace Affinity (LSA) [31] [6] on the same database. Figure 3 gives two histograms of the misclassification rates over the sequences with two and three motions, respectively. There are several other algorithms that have been tested on the Hopkins155 database (GPCA, RANSAC etc.), but we list these two algorithms because they have to date *the best* reported misclassification rates in many categories of sequences.

As these results show, ALC performs well compared to the state-of-the-art. It has the best overall misclassification rate as well as for the checkerboard sequences. In categories where ALC is not the best, its performance is still competitive. The one notable exception is for the set of articulated sequences. As ALC typically needs the samples for a group to cover the subspace with sufficient density, there would have to be a large number of tracked features of an articulated motion for ALC to correctly segment it. However, in the Hopkins155 database many of the scenes with articulated motions are in fact scenes of human motion with only a few tracked

[6]For LSA we report the results for the version that projects the data onto a $4N$-dimensional space.

(a) Misclassification Rates (%).

Checkerboard	MSL	LSA	ALC_5	ALC_{sp}
Average	5.94%	3.38%	3.61%	**2.37%**
Median	0.00%	0.57%	0.00%	0.31%
Traffic	MSL	LSA	ALC_5	ALC_{sp}
Average	**2.15%**	9.05%	3.05%	3.06%
Median	0.00%	1.96%	0.92%	1.35%
Articulated	MSL	LSA	ALC_5	ALC_{sp}
Average	6.53%	**4.58%**	6.95%	12.30%
Median	0.00%	1.22%	0.89%	0.95%
All Sequences	MSL	LSA	ALC_5	ALC_{sp}
Average	5.06%	4.87%	3.76%	**3.37%**
Median	0.00%	0.90%	0.26%	0.49%

(b) Average computation times. Results in parentheses for ALC use the rank-1 Cholesky update discussed in §II-B.

Method	MSL	LSA	ALC_5	ALC_{sp}
Checkerboard	17h 40m	10.423s	12m 6s (6m 5s)	24m 4s (7m 12s)
Traffic	12h 42m	8.433s	8m 42s (4m 15s)	17m 19s (4m 56s)
Articulated	7h 35m	3.551s	4m 51s (2m 16s)	10m 43s (2m 40s)
All Sequences	19h 11m	9.474s	10m 32s (5m 15s)	21m 3s (6m 11s)

TABLE II

PERFORMANCE OVER ENTIRE HOPKINS155 DATABASE.

features.

In terms of computation time, we see that the algorithms fall into three categories: the spectral method LSA runs on the order of seconds, our agglomerative methods run on the order of minutes, and the iterative method MSL runs on the order of hours. Keep in mind that our methods are run for 101 different choices of the parameter ε. Also, by using the rank-1 Cholesky update, both ALC_5 and ALC_{sp} run two to four times faster on each sequence. Finally, with regard to the projection dimension, our results indicate that, overall, ALC_{sp} performs better than ALC_5.

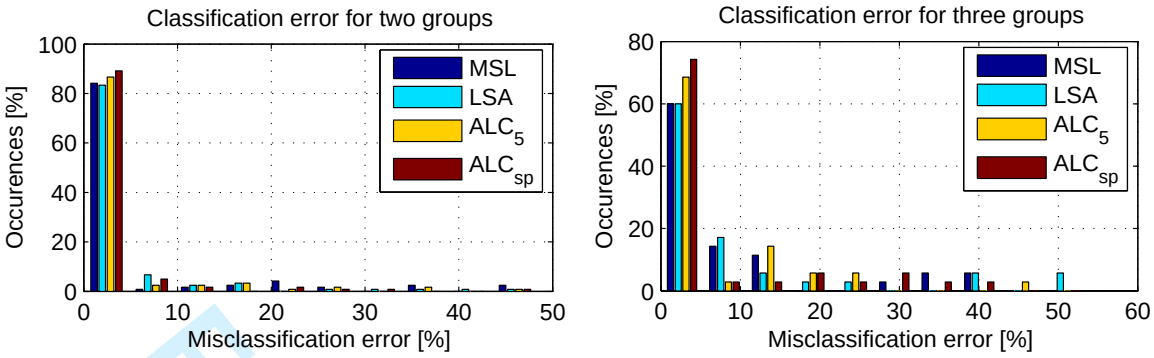

Fig. 3. Misclassification rate histograms for various algorithms on the Hopkins155 database.

III. Robust Subspace Separation

In this section, we show how to make subspace separation robust to the three kinds of pathologies discussed earlier. In particular, we show that ALC naturally deals with outliers, and, by harnessing the low-dimensional subspace structure of the data, we can repair incomplete and corrupted samples *prior* to subspace separation.

A. Outlying Trajectories

Dynamic scenes often contain trajectories that do not correspond to any of the motion models in the scene. Such trajectories can arise from motions not well described by the affine camera model, such as the motion of non-rigid objects. These kinds of trajectories have been referred to as "sample outliers" by [7], suggesting that no subset of the trajectory corresponds to any affine motion model. Fortunately, ALC deals with such sample outliers in an elegant fashion. In [20], it was observed that in low-dimensional spaces, a sufficient number of outliers will cover the entire space, and so the algorithm tends to group all outliers into a single group. Such a group can be easily detected, because the number of bits per vector in that group will be very large relative to other groups. However, in higher-dimensional spaces, such as in our motion segmentation problem, it would require an enormous number of outliers to fill the space. If outliers are thinly scattered in the ambient space, they will be most efficiently encoded when each outlier is its own group. Such small groups are also easily detectable.

Experiments with Simulated Outliers. We choose three representative sequences from the

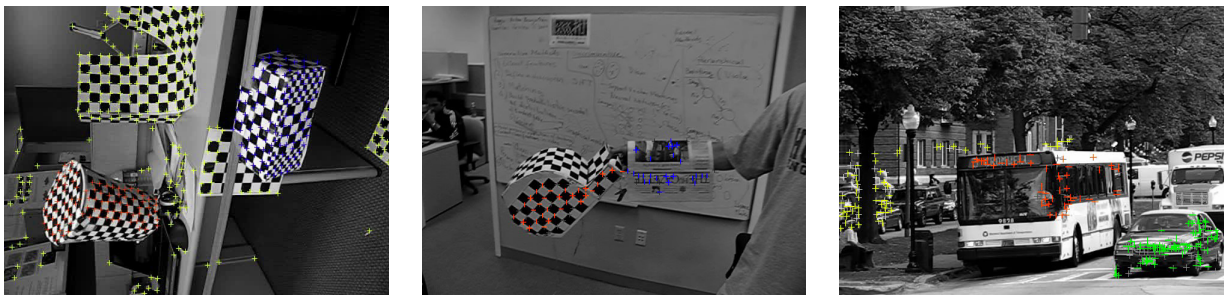

(a) 1R2RC sequence (b) arm sequence (c) cars10 sequence

Fig. 4. Three motion sequences from the Hopkins155 database [24].

Hopkins155 database for simulation: "1R2RC" (checkerboard), "arm" (articulation), and "cars10" (traffic) (see Figure 4). We compare the robustness to sample outliers of ALC[7] and Local Subspace Affinity (LSA) [31], a spectral clustering-based motion segmentation algorithm that is reasonably robust to outliers. We add between 0% and 25% outlying trajectories to the dataset of a given motion sequence. Outlying trajectories were generated by choosing a random initial point in the first frame, and then performing a random walk to neighboring pixels through the following frames. Each increment is generated by taking the difference between the coordinates of a randomly chosen point in two randomly chosen consecutive frames. In this way the outlying trajectories will qualitatively have the same statistical properties as the other trajectories, but will not obey to any particular motion model. We then input these outlier-ridden datasets into LSA and ALC, respectively, and compute the misclassification rate and outlier detection rate for both algorithms.[8] For each experiment we run 100 trials with different randomly generated outlying trajectories. Table III shows the average misclassification rates and outlier detection rates for each experiment. As the results show, ALC can easily detect outliers without hindering motion segmentation, whereas for LSA, the outliers tend to interfere with the classification of valid trajectories. Hence, for subsequent experiments in this paper, we will not compare our methods with LSA.

Experiments with Real Outliers. We apply ALC to four motion sequences with real outlying

[7]For this simulation, we use ALC_5 , the version of ALC that projects the data onto a 5-dimensional space.

[8]In ALC a trajectory is labeled an outlier if it belongs to a group with less than five samples. In our implementation of LSA, a trajectory is labeled as an outlier if its distance from the nearest motion subspace is greater than a predetermined threshold.

(a) Misclassification Rates

	1R2RC [%]		arm [%]		cars10 [%]	
[%]	LSA	ALC	LSA	ALC	LSA	ALC
0	2.40	**1.09**	22.08	**0.00**	16.84	**1.34**
7	6.91	**1.29**	24.17	**0.13**	31.97	**0.40**
15	3.09	**1.31**	15.38	**0.06**	26.43	**0.19**
25	2.69	**1.16**	10.25	**0.04**	24.59	**0.17**

(b) Outlier Detection Rates

	1R2RC [%]		arm [%]		cars10 [%]	
[%]	LSA	ALC	LSA	ALC	LSA	ALC
0	98.04	100	77.9	100	86.87	100
7	94.75	99.99	92.79	100	96.82	99.70
15	98.04	99.98	91.34	100	98.84	99.81
25	98.20	99.97	95.56	100	98.76	99.83

TABLE III

MISCLASSIFICATION AND OUTLIER DETECTION RATES FOR LSA AND ALC AS A FUNCTION OF THE OUTLIER PERCENTAGE (FROM 0% TO 25%) FOR THREE MOTION SEQUENCES IN FIGURE 4.

(a) books sequence

(b) carsbus3 sequence

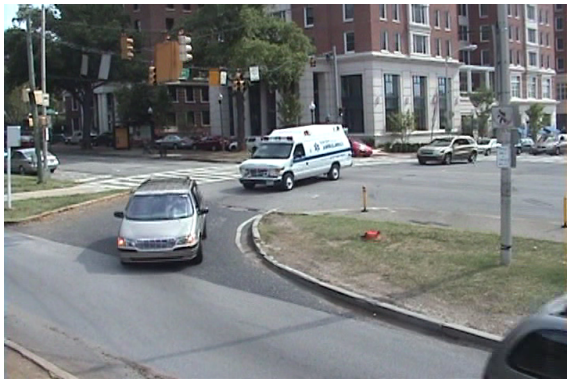

(c) carsTurning sequence

(d) nrbooks3 sequence

Fig. 5. Example image frames from four motion sequences containing real outlying trajectories.

trajectories shown in Figure 5. For each sequence, trajectories were obtained with an automatic tracker, and the ground-truth segmentation was manually determined. A trajectory was termed an inlier if it is correctly tracked in all frames, and an outlier if it is incorrectly tracked in all frames.[9] Information about the number of motions, samples for each group, and the number of outliers in each sequence are listed in Table IV.

The Misclassification and Outlier Detection rates are listed in Table V. As these results show, ALC_{sp} is able to detect and remove real outliers without substantially affecting segmentation of inliers, while ALC_5 is not. The one exception is the "carsbus3" sequence, where ALC_5 seems to outperform ALC_{sp}. However, qualitatively examining the segmentation results, we see that ALC_{sp} achieves its 9.74% misclassification rate by falsely grouping some outliers with features from the car in the foreground. However, these trajectories are fairly close to the car, so it could be argued that they are in fact, noisy or corrupted trajectories rather than outliers. On the other hand, ALC_5 gets its low misclassification rate of 1.62% by falsely rejecting most of the trajectories from that same car as outliers. This experiment suggests, that to reliably segment motion data in the presence of outliers, the data should be projected into a space with more than just five dimensions.

Sequence	# motions	# samples	# outliers
books	5	45, 41, 28, 71, 30	127
carsbus3	3	85, 45, 89	89
carsTurning	4	51, 114, 52, 517	43
nrbooks3	3	129, 168, 91	35

TABLE IV

INFORMATION ABOUT THE FOUR MOTION SEQUENCES IN FIGURE 5 CONTAINING REAL OUTLYING TRAJECTORIES (NUMBERS OF MOTIONS, SAMPLES FOR EACH GROUP AND OUTLIERS)

[9]For this experiment, trajectories with partial corruption were removed from the dataset. This is because trajectories with partial corruption still retain a valid class label. Thus it is better to deal with such trajectories as incomplete or corrupted, which we will discuss in §III-B and §III-C.

	books [%]		carsbus3 [%]		carsTurning [%]		nrbooks3 [%]	
	ALC_5	ALC_{SP}	ALC_5	ALC_{SP}	ALC_5	ALC_{SP}	ALC_5	ALC_{SP}
Misclassification Rate	7.89	**2.05**	**1.62**	9.74	15.44	**0.26**	11.11	**0.47**
Outlier Detection Rate	98.25	99.42	76.95	100	75.16	97.04	27.66	98.58

TABLE V

MISCLASSIFICATION AND OUTLIER DETECTION RATES FOR ALC_5 AND ALC_{SP} ON FOUR MOTION SEQUENCES WITH REAL OUTLYING TRAJECTORIES.

B. Incomplete Trajectories

In practice, due to occlusions or limitations of the tracker, some features may be missing in some image frames and lead to incomplete trajectories in $\mathtt{Y}$. There are many methods in the computer vision literature for filling in the missing entries of a matrix of motion trajectories [15], [14], [19]. These methods typically assume that the data matrix is low rank. For a matrix with low column rank, the problem of completing missing data can in fact be cast as a rank minimization problem:

$$\hat{\mathtt{Y}} = \underset{\mathtt{X}}{\operatorname{argmin}} \operatorname{rank}(\mathtt{X}) \quad \text{subject to} \quad \mathcal{M}(\mathtt{X}) = \mathcal{M}(\mathtt{Y}), \tag{11}$$

where $\mathcal{M}(\cdot)$ is a mask that matches given entries in $\mathtt{Y}$. As we mentioned earlier, rank minimization is a difficult problem and most of the methods in computer vision mentioned above rely on an iterative alternative minimization scheme. There has been a significant breakthrough in the compressed sensing literature that shows that the above problem can be solved correctly and efficiently by semi-definite programming when the rank is low enough. In fact, a very sharp bound is derived for how many entries are needed for an exact completion of the matrix [2].[10]

However, these powerful tools for entry completion run into serious problems when the columns of the data matrix are from multiple subspaces. Data drawn from a union of subspaces can potentially be full rank – the matrix $\hat{\mathtt{Y}}$ is often over-complete. As such, the problem becomes

[10]According to this new result, rather surprising, the percentage of entries needed for an exact completion goes to zero as the dimension goes to infinity, whereas for the iterative schemes, such as Power Factorization [15], the conventional rule of thumb is that one needs about at least 20% to 30% entries for a good chance of success.

extremely *underdetermined* as there is in general no unique solution for the values of the missing entries as linear combination of the known entries. However, by harnessing the low-dimensional multiple-subspace structure of the data set, it is actually possible to *complete* these trajectories *prior* to subspace separation.

The key observation is that samples drawn from a low-dimensional linear subspace are *self-expressive*, meaning that a sample can be expressed in terms of a few other samples from the same linear subspace. More precisely, if the given sample is $\boldsymbol{y} \in \mathbb{R}^D$ and $\mathtt{Y} \in \mathbb{R}^{D \times P}$ is the data matrix whose columns are all of the *other* samples in the dataset, then there exists a coefficient vector $\boldsymbol{c} \in \mathbb{R}^P$ that satisfies

$$\boldsymbol{y} = \mathtt{Y}\boldsymbol{c}. \tag{12}$$

As the number of samples P is usually much greater than the dimension of the ambient space D, (12) is a highly underdetermined system of linear equations, and so, in general, $\boldsymbol{c}$ is not unique. In fact, any D vectors in the set that span $\mathbb{R}^D$ can serve as a basis for representing $\boldsymbol{y}$. However, since $\boldsymbol{y}$ lies in a low-dimensional linear subspace, it can be represented as a linear combination of only a few vectors from the same subspace. Hence, its coefficient vector should have only a few nonzero entries corresponding to vectors from the same subspace. Thus, what we seek is the *sparsest* $\boldsymbol{c}$:

$$\boldsymbol{c}^* = \underset{\boldsymbol{c}}{\operatorname{argmin}} \|\boldsymbol{c}\|_0 \quad \text{subject to} \quad \boldsymbol{y} = \mathtt{Y}\boldsymbol{c}, \tag{13}$$

where $\|\cdot\|_0$ is the "ℓ^0 norm", equal to the number of nonzero entries in the vector. The sparsest coefficient vector $\boldsymbol{c}^*$ is unique when $\|\boldsymbol{c}^*\|_0 < D/2$. In the general case, ℓ^0 minimization, like MRM, is known to be NP-Hard[11]. Fortunately, due to the findings of Donoho et al. [8], it is known that if $\boldsymbol{c}^*$ is sufficently sparse (i.e. $\|\boldsymbol{c}^*\|_0 \lesssim \lfloor \frac{D+1}{3} \rfloor$), then the ℓ^0 minimization in (13) is equivalent to the following ℓ^1 minimization:

$$\boldsymbol{c}^* = \underset{\boldsymbol{c}}{\operatorname{argmin}} \|\boldsymbol{c}\|_1 \quad \text{subject to} \quad \boldsymbol{y} = \mathtt{Y}\boldsymbol{c}, \tag{14}$$

which is essentially a linear program.

We apply these results to the problem of dealing with incomplete data. Suppose we have a sample $\boldsymbol{y} \in \mathbb{R}^D$ with missing entries $\{y_i\}_{i \in I}, I \subset \{1, \ldots, D\}$ and a dataset $\mathtt{Y} \in \mathbb{R}^{D \times P}$ with *no*

[11] In fact, when MRM is applied to a set of *diagonal* matrices, it reduces to ℓ^0 minimization.

missing entries. The idea is to use the available entries in $\boldsymbol{y}$ and the corresponding rows in $\mathtt{Y}$ to complete the vector. Let $\hat{\boldsymbol{y}} \in \mathbb{R}^{D-|I|}$ and $\hat{\mathtt{Y}} \in \mathbb{R}^{(D-|I|)\times P}$ be $\boldsymbol{y}$ and $\mathtt{Y}$ with the rows indexed by I removed, respectively. By removing these rows, we are essentially projecting the data onto the $(D-|I|)$-dimensional subspace orthogonal to $\text{span}(\{\boldsymbol{e}_i : i \in I\})$, where $\boldsymbol{e}_i$ is the i-th vector in the canonical basis for $\mathbb{R}^D$. This is licit because, as long as the dimension of each subspace is strictly less than $d = (D-|I|)$, an arbitrary d-dimensional projection preserves the structural relationships between the subspaces with probability one. Thus if we solve the linear program[12]:

$$\boldsymbol{c}^* = \underset{\boldsymbol{c}}{\text{argmin}} \, \|\boldsymbol{c}\|_1 \quad \text{subject to} \quad \hat{\boldsymbol{y}} = \hat{\mathtt{Y}}\boldsymbol{c}, \tag{15}$$

then the completed vector $\boldsymbol{y}^*$ can be recovered as

$$\boldsymbol{y}^* = \mathtt{Y}\boldsymbol{c}^*. \tag{16}$$

Experiments with simulated missing data. We now test the accuracy of our ℓ^1-based method for entry completion. In each trial, we randomly select a trajectory $\boldsymbol{y}_p$ from the dataset for a given sequence, and remove $1 \leq m \leq D-1 = 2F-1$ of its entries. We then apply (15) and (16) to recover the missing entries[13]. In order to simulate many trajectories with missing entries in the dataset, we perform 5 different experiments. In each experiment, we use a subset $\mathtt{Y}_c$ containing between 20% to 100% of the remaining trajectories to complete $\boldsymbol{y}_p$.

We also compare the performance of our method with Power Factorization [15], an iterative technique that has been applied to incomplete motion data [27]. Note that the two approaches work under different operating conditions. Our ℓ^1-based approach uses a set of complete vectors to fill in the missing entries of incomplete vectors, *one* vector at a time. Power Factorization fills in the entries of *all* incomplete vectors simultaneously, but relies on a low-rank representation for the whole matrix. For fair comparison, we embed the trajectories in a data matrix $\mathtt{Y}$, and then randomly remove m entries from $\boldsymbol{y}_p$ as well as each column of $\mathtt{Y} \setminus \mathtt{Y}_c$. We then apply Power Factorization to $\mathtt{Y}$ to fill in its missing entries, subject to a rank constraint of $r = 4N$, where N is the number of motions in the scene.

[12] As suggested in [30], one can deal with noisy data by replacing the equality constraint in (15) with $\|\hat{\boldsymbol{y}} - \hat{\mathtt{Y}}\boldsymbol{c}\|_2 \leq \varepsilon$. Though no longer a linear program, the problem can still be solved efficiently via semidefinite programming.

[13] For all of our experiments that use ℓ^1-minimization, we use the freely available CVX toolbox for MATLAB [13].

Figure 6 shows the results for 200 trials. For each method and each sequence, we plot the average per-entry error of the recovered trajectory $\hat{\boldsymbol{y}}_p$ with respect to the ground truth versus the percentage of missing entries in each incomplete trajectory. The different colored plots are for the experiments with varying percentage of the dataset used for completion. For all motion sequences, our method is able to reconstruct trajectories to within subpixel accuracy even with over 80% of the entries missing! The performance of both methods remains consistent even when the entries are completed with small subsets of the remaining data. This suggests that both methods can work well even if a large number of trajectories have missing features. However, as these simulations show, our method clearly outperforms Power Factorization, obtaining, lower per-entry error and converging for a larger percentage of missing entries. This is because our method takes advantage of the multiple-subspace structure in the data, while Power Factorization does not.

Experiments with real missing data. We now test our robust subspace separation method on real motion sequences with incomplete or corrupted trajectories. We first use the three motion sequences shown in Figure 7. These sequences are taken from [27] and are similar to the checkerboard sequences in Hopkins155. Each sequence contains three different motions and was split into three new sequences containing only trajectories from the first and second groups, first and third groups, and second and third groups, respectively. Thus, in total, we have twelve motion sequences, nine with two motions, and three with three motions. For these sequences, between 4% and 35% of the entries in the data matrix of trajectories are corrupted. These entries were manually located and labeled.

To see how ℓ^1-based entry completion affects the quality of segmentation, we remove the entries of trajectories that were marked as corrupted so that we may treat them as missing entries. We apply our ℓ^1-based entry completion method to this data, and input the completed data into ALC_5 and ALC_{sp}, respectively. For comparison, we also use Power Factorization and Robust PCA [7] to complete the data before segmentation. The misclassification rate for each sequence is listed in Table V(a). Our ℓ^1-based approach performs competitively with both Power Factorization and Robust PCA. The average performance of ℓ^1+ALC_5 is skewed by its misclassification rate for the "oc2R3RCRT" sequence. This is likely an artifact of the method we use to choose ε. Notice that while both Robust PCA and Power Factorization work well when

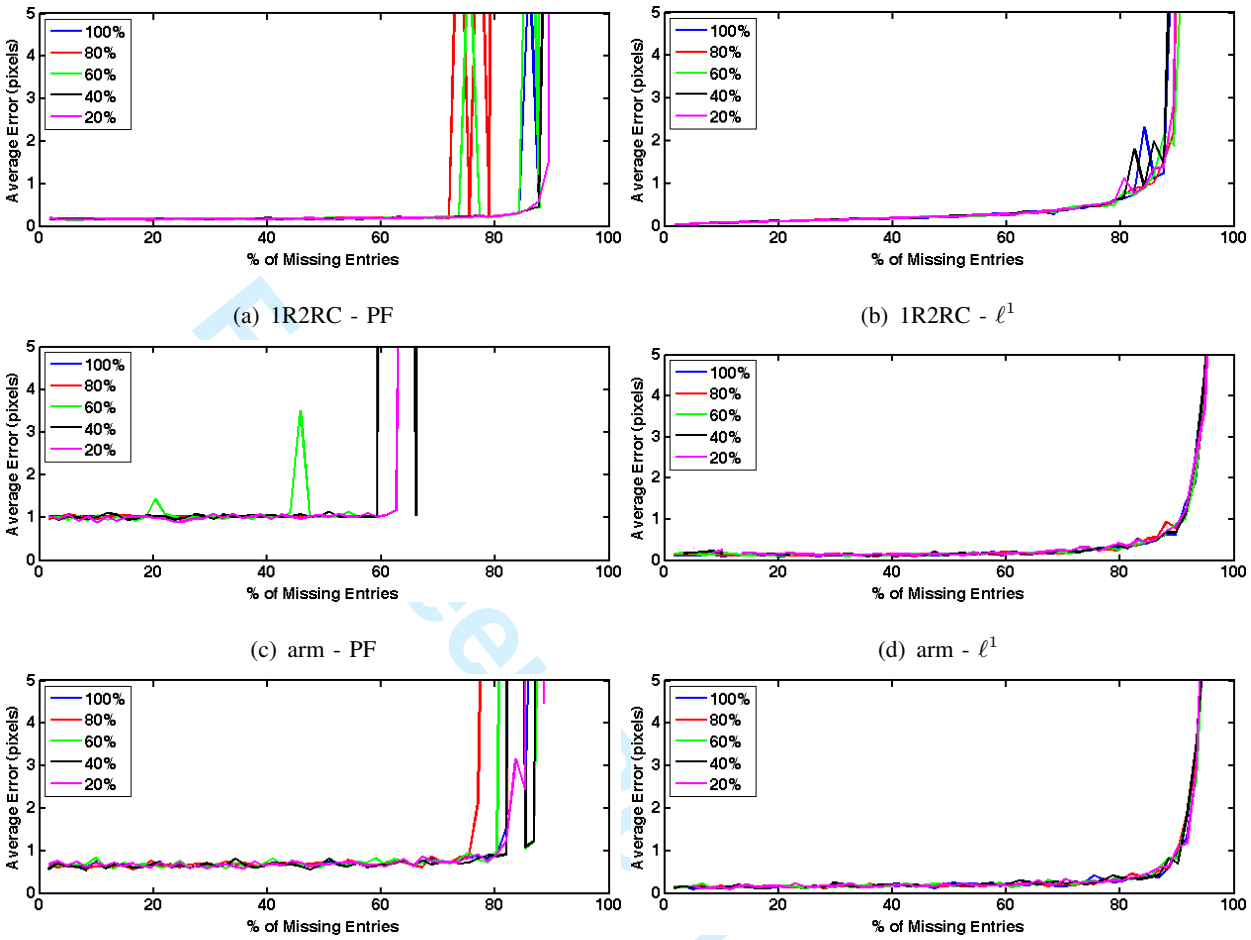

(a) 1R2RC - PF (b) 1R2RC - ℓ^1

(c) arm - PF (d) arm - ℓ^1

(e) cars10 - PF (f) cars10 - ℓ^1

Fig. 6. Errors on the recovered trajectories using our ℓ^1-based trajectory completion for the sequences: "1R2RC", "arm", and "cars10". The different colored plots are for experiments with varying percentage of the dataset used for completion.

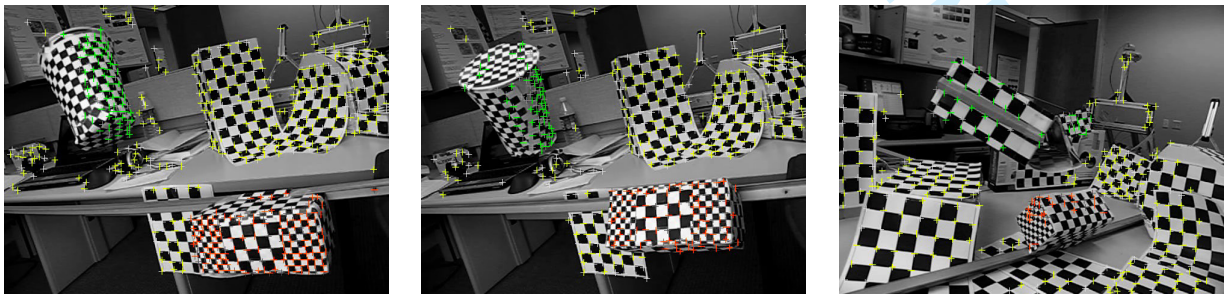

(a) oc1R2RC (b) oc1R2RCT (c) oc2R3RCRT

Fig. 7. Example frames from three motion sequences with incomplete or corrupted trajectories. Sequences taken from [27].

combined with ALC_5 , their performance degrades significantly when combined with ALC_{sp}. Thus, alternative minimization techniques like Power Factorization and Robust PCA tend to work well only when the dimensionality of projection is small.

(a) Misclassification Rates

	PF		RPCA		ℓ^1	
[%]	ALC_5	ALC_{sp}	ALC_5	ALC_{sp}	ALC_5	ALC_{sp}
oc1R2RC	**0.15**	6.25	**0.15**	2.28	**0.15**	**0.15**
oc1R2RC_g12	8.79	14.01	**0.00**	8.79	**0.00**	**0.00**
oc1R2RC_g13	**0.00**	1.02	3.67	7.76	**0.00**	**0.00**
oc1R2RC_g23	**0.19**	1.75	**0.19**	1.55	**0.19**	**0.19**
oc1R2RCT	1.82	3.45	2.00	6.91	**0.91**	1.27
oc1R2RCT_g12	**0.00**	15.15	0.43	14.28	0.87	0.87
oc1R2RCT_g13	5.16	2.58	0.94	7.75	**0.70**	1.41
oc1R2RCT_g23	3.39	3.61	0.45	2.48	**0.00**	0.90
oc2R3RCRT	**2.36**	21.20	2.36	27.62	42.40	2.57
oc2R3RCRT_g12	**0.00**	34.57	**0.00**	41.36	**0.00**	1.23
oc2R3RCRT_g13	**0.51**	16.62	**0.51**	21.74	**0.51**	4.35
oc2R3RCRT_g23	0.26	9.45	**0.00**	22.83	**0.00**	2.36
Average	1.89	10.81	**0.89**	13.78	3.81	1.28
Median	0.39	7.85	0.44	8.27	0.17	1.07

(b) Misclassification Rates

	PF		RPCA		ℓ^1	
[%]	ALC_5	ALC_{sp}	ALC_5	ALC_{sp}	ALC_5	ALC_{sp}
books	**0.00**	1.88	0.13	**0.00**	0.75	**0.00**
carsbus3	**0.00**	**0.00**	15.60	**0.00**	**0.00**	**0.00**
carsTurning	15.03	1.44	**0.00**	0.85	16.07	**0.00**
nrbooks3	10.05	**0.00**	5.52	**0.00**	5.19	**0.00**

(c) Outlier Detection Rates

	PF		RPCA		ℓ^1	
[%]	ALC_5	ALC_{sp}	ALC_5	ALC_{sp}	ALC_5	ALC_{sp}
books	57.06	63.09	40.65	44.03	76.84	91.34
carsbus3	74.79	93.59	77.68	75.22	74.36	100.00
carsTurning	78.06	76.00	74.47	94.04	65.29	98.35
nrbooks3	52.51	76.18	37.50	75.29	62.89	87.52

TABLE VI

COMPARISON OF POWER FACTORIZATION AND ROBUST PCA WITH OUR ℓ^1-BASED APPROACH FOR REAL MOTION SEQUENCES WITH INCOMPLETE DATA. LEFT: MISCLASSIFICATION RATES FOR THE 12 SEQUENCES IN FIGURE 7. RIGHT: MISCLASSIFICATION AND OUTLIER DETECTION RATES FOR THE 4 SEQUENCES IN FIGURE 5.

We also test our Power Factorization, Robust PCA, and our ℓ^1-based approach on the four motion sequences in Figure 5. In this experiment, we remove the outlying trajectories from each sequence and instead use the partially corrupted trajectories. Each trajectories has between 0% and 75% of its entries missing. The number and location of missing entries for each trajectory was manually determined. These sequences contain many corrupted trajectories, and so it is possible that an incomplete trajectory cannot be satisfactorily completed, and will likely be classified as an outlier. Thus, to get a sense of how well the entries of incompete trajectories are filled

in, we compute both the misclassification rate *and* the outlier detection rate for each sequence. The results are listed in Tables V(b) and V(c). For all four sequences, our ℓ^1-based approach in conjunction with ALC_{SP} can effectively deal with incomplete trajectories, treating the fewest as possible as outliers. For the cases where RPCA+ALC or PF+ALC achieves low misclassification rates, notice the outlier detection rate is also low. This suggests that these iterative methods were unable to recover the missing entries of the incomplete trajectories, and so such trajectories are incorrectly rejected as outliers.

C. Corrupted Trajectories

Corrupted entries can be present in a trajectory when the tracker unknowingly loses track of feature points[14]. Such entries are gross errors that could have arbitrary magnitude. One could treat corrupted trajectories as sample outliers.[15] However, in a corrupted trajectory, a portion of the entries still corresponds to a motion in the scene, hence it seems wasteful to simply discard such information.

Repairing a vector with corrupted entries is a much more difficult problem than the entry completion problem in §III-B, because both the number and location of the corrupted entries in the vector are *not known*. Once again, by taking advantage of the low-dimensional multi-subspace structure of the dataset, we can both detect and repair vectors with corrupted entries *prior* to subspace separation.

A corrupted vector $\hat{\boldsymbol{y}}$ can be modeled as

$$\hat{\boldsymbol{y}} = \boldsymbol{y} + \boldsymbol{e}, \tag{17}$$

where $\boldsymbol{y}$ is the uncorrupted vector, and $\boldsymbol{e} \in \mathbb{R}^D$ is a vector that contains all of the gross errors. We assume that there are only a few gross errors, so $\boldsymbol{e}$ will only have a few nonzero entries, and thus be sparse[16]. As long as there are enough uncorrupted vectors in the dataset, we can

[14]These kind of trajectories are called "intra-sample outliers" in [7].

[15]Indeed, if a dataset with some corrupted trajectories is input to ALC, the algorithm will classify those trajectories as outliers, as the gross errors will greatly increase the coding length of their ground-truth motion group.

[16]We realize that, in practice, trajectories may be corrupted by a large number of gross errors. However, it is unlikely that *any* method can repair such trajectories, and so it is best to treat them as sample outliers.

express $\boldsymbol{y}$ as a linear combination of the other vectors in the dataset as in §III-B. If $\mathtt{Y} \in \mathbb{R}^{P \times D}$ is a matrix whose columns are the other vectors in the dataset, then (17) becomes

$$\hat{\boldsymbol{y}} = \mathtt{Y}\boldsymbol{c} + \boldsymbol{e} = \begin{bmatrix} \mathtt{Y} & \mathtt{I} \end{bmatrix} \begin{bmatrix} \boldsymbol{c} \\ \boldsymbol{e} \end{bmatrix} \doteq \mathtt{B}\boldsymbol{w}. \tag{18}$$

We would like both the coefficient vector $\boldsymbol{c}$ and the error vector $\boldsymbol{e}$ to be sparse[17]. If the true $\boldsymbol{c}$ and $\boldsymbol{e}$ are sufficiently sparse, we can simultaneously find the sparsest $\boldsymbol{c}$ and $\boldsymbol{e}$ by solving the linear program:

$$\boldsymbol{w}^* = \underset{\boldsymbol{w}}{\operatorname{argmin}} \|\boldsymbol{w}\|_1 \quad \text{subject to} \quad \hat{\boldsymbol{y}} = \mathtt{B}\boldsymbol{w}. \tag{19}$$

The convex optimization problem in (19) has been successfully applied to robust face recognition in the presence of occlusion [30], and is provably optimal for certain types of corruption [28]. Once $\boldsymbol{w}^*$ is computed, we decompose it into $\boldsymbol{w}^* = \begin{bmatrix} \boldsymbol{c}^* & \boldsymbol{e}^* \end{bmatrix}^T$, where $\boldsymbol{c}^* \in \mathbb{R}^P$ is the recovered coefficient vector and $\boldsymbol{e}^* \in \mathbb{R}^D$ is the recovered error vector. The repaired vector $\boldsymbol{y}^*$ is simply

$$\boldsymbol{y}^* = \mathtt{Y}\boldsymbol{c}^*. \tag{20}$$

The error vector $\boldsymbol{e}^*$ also provides useful information. The nonzero entries of $\boldsymbol{e}^*$ are precisely the gross errors in $\hat{\boldsymbol{y}}$.

Experiments with simulated corrupted data. We now test the limits of our ℓ^1-based method for repair of corrupted trajectories. For each trial in the experiments, we randomly select a trajectory $\boldsymbol{y}_p$ from the given dataset, and randomly *select and corrupt* between 1 and $D - 1 = 2F - 1$ entries in the vector. To corrupt the selected entries, we *replace* them with random values drawn from a distribution that is uniform in the pixel coordinate space. We then apply (19) and (20) to both detect the locations of corrupted entries, as well as repair them. In each experiment we run 200 trials and average the errors. We perform five experiments of this type, each with a portion (from 0% to 80%) of the remaining dataset $\mathtt{Y}$ being corrupted in the same way as $\boldsymbol{y}_p$. The results of these experiments are shown in Figure 8 (bottom). For each sequence, we plot the average per-entry error of the repaired vector with respect to the ground truth versus the percentage of corrupted entries in each vector. The different colors represent experiments with

[17]The columns of $\mathtt{Y}$ should be scaled to have unit ℓ^2 norm to ensure that no vector is preferred in the sparse representation of $\boldsymbol{w}$.

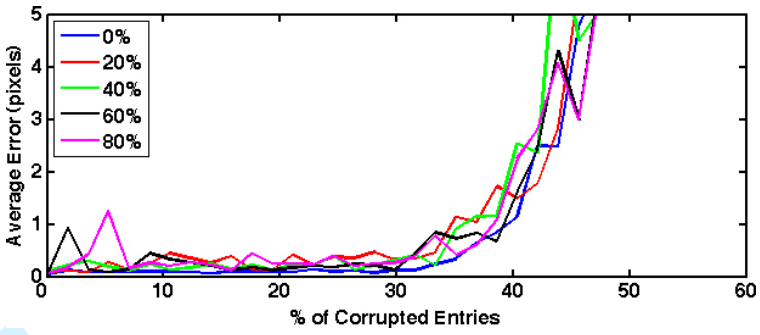

(a) 1R2RC sequence

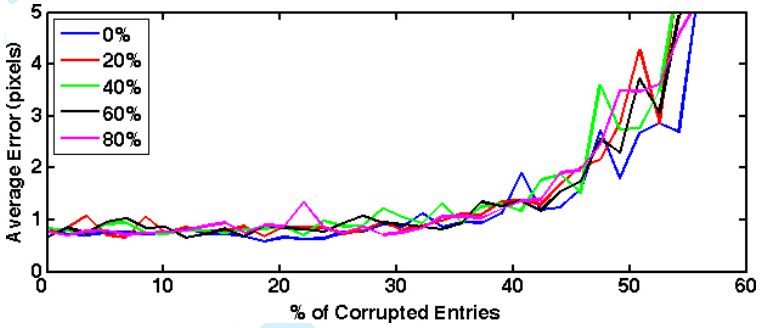

(b) arm sequence

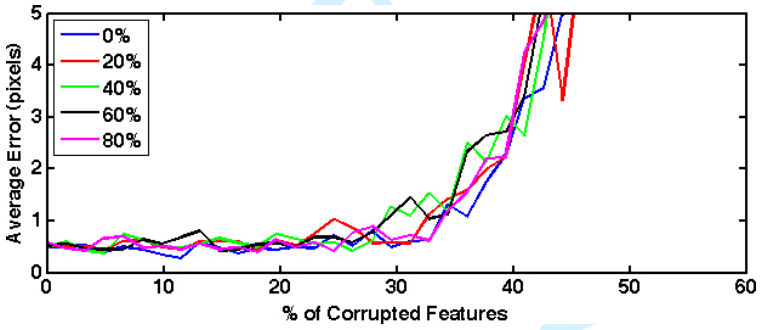

(c) cars10 sequence

Fig. 8. Results for our ℓ^1-based detection and repair of corrupted trajectories for the sequences: "1R2RC" (top), "arm" (center), and "cars10" (bottom). The different colors represent experiments with varying percentage of corrupted trajectories in the dataset.

varying portions of corrupted $\mathtt{Y}$. As Figure 8 shows, this method is able to reconstruct vectors to within subpixel accuracy even with roughly 1/3 of the entries corrupted. This is in line with the bound $\|\boldsymbol{c}^*\|_0 < \lfloor \frac{D+1}{3} \rfloor$ given by [8]. We also see that the performance remains consistent even if 80% of the entire dataset is corrupted!

Experiments with real corrupted data. We test our ability to repair corrupted trajectories, and observe the effects of the repair on segmentation. We apply our ℓ^1-based repair and detection

method to the raw motion sequences in Figure 7, and then input the *repaired* data to ALC_5 and ALC_{sp}, respectively. For comparison, we also use Robust PCA to complete the data before segmentation. The misclassification rate for each sequence is listed in Table VII (left). Both Robust PCA and our ℓ^1-based approach can repair corrupted trajectories to achieve reasonable segmentations.

We also test our ℓ^1-based approach for error corrections on the four motion sequences in Figure 5. In this experiment, each trajectory has between 0% and 25% of its entries corrupted. The misclassification and outlier detection rates for each sequence are listed in Table VII (right). For these more realistic sequences we see that our ℓ^1-based approach can still effectively deal with corrupted trajectories, treating the fewest as possible as outliers. For the cases where RPCA+ALC achieves good misclassification rates, notice the outlier detection is also low, meaning that Robust PCA was unable to detect and correct the errors in the corrupted trajectories. Finally, in both of these experiments, we note that both methods tend to work better when combined with ALC_{sp}.

IV. Conclusions and Future Work

In this paper, we have investigated the problem of motion segmentation from the perspective of robust subspace separation. We have shown that the key for correct segmentation, data completion, and error correction is to correctly harness the intrinsic low-dimensional, sparse structures within such data. This has made the proper choice of measures for sparsity and compactness the central issue. We have shown that in our context, both the (lossy) coding length and 1-norm are good surrogates for the matrix rank and vector sparsity, respectively. Not only is the use of these measures theoretically well-founded, but also we have demonstrated with extensive simulations and experiments that they indeed lead to algorithms with superior performance for segmenting motion trajectories despite outliers, incomplete data, and random errors. The proposed techniques and algorithms are in fact generic to subspace separation, and can conceivably be used in other application domains with little modification.

This paper provides strong, encouraging empirical evidence for people to work on many exciting open theoretical problems. In this paper, we have explored several schemes for both improving the speed and convergence of the coding-length based agglomerative algorithm. In the algorithm, the coding length is used as a "distance" measure between pairs of subsets. It is worth investigating if such a measure exhibits *locality-sensitive hashing* properties [6] as other

(a) Misclassification Rates

	RPCA		ℓ^1	
[%]	ALC_5	ALC_{sp}	ALC_5	ALC_{sp}
oc1R2RC	1.68	**0.15**	**0.15**	**0.15**
oc1R2RC_g12	**0.00**	2.61	**0.00**	**0.00**
oc1R2RC_g13	**0.00**	0.20	**0.00**	**0.00**
oc1R2RC_g23	0.19	**0.00**	0.19	**0.00**
oc1R2RCT	8.36	1.64	**0.91**	1.45
oc1R2RCT_g12	0.43	**0.00**	**0.00**	0.43
oc1R2RCT_g13	0.47	1.88	**0.23**	1.64
oc1R2RCT_g23	0.19	**0.00**	**0.00**	1.35
oc2R3RCRT	42.61	**7.49**	41.97	9.64
oc2R3RCRT_g12	0.62	0.62	0.62	**0.00**
oc2R3RCRT_g13	3.83	9.97	**2.81**	8.95
oc2R3RCRT_g23	6.56	9.97	**2.89**	12.60
Average	5.66	**3.01**	4.15	3.02
Median	1.15	1.61	0.21	0.89

(b) Misclassification Rates

	RPCA		ℓ^1	
[%]	ALC_5	ALC_{sp}	ALC_5	ALC_{sp}
books	21.58	3.08	2.78	**0.00**
carsbus3	**0.00**	**0.00**	**0.00**	**0.00**
carsTurning	14.02	**0.00**	17.95	**3.67**
nrbooks3	3.25	**0.00**	6.45	**0.00**

(c) Outlier Detection Rates

	RPCA		ℓ^1	
[%]	ALC_5	ALC_{sp}	ALC_5	ALC_{sp}
books	30.16	36.60	85.19	83.95
carsbus3	62.13	95.32	78.83	100.00
carsTurning	95.32	76.66	72.82	97.72
nrbooks3	6.20	65.29	66.73	82.26

TABLE VII

COMPARISON OF ROBUST PCA WITH OUR ℓ^1-BASED APPROACH FOR REAL MOTION SEQUENCES WITH CORRUPTED DATA. LEFT: MISCLASSIFICATIONS RATE FOR THE 12 REAL SEQUENCES IN FIGURE 7. RIGHT: MISCLASSIFICATION AND OUTLIER DETECTION RATES FOR THE 4 SEQUENCES IN FIGURE 5.

norms so that more principled speedup algorithms can be derived.

We have seen that typically the agglomerative algorithm converges to the correct motion segmentation for a wide range of choice of ε. There is still a lack of proof for under what conditions the agglomerative algorithm is expected to converge to the segmentation with *globally* minimum coding length. This remains an open problem that we will investigate in the future.

Although the problem of completing a low-rank matrix has recently been solved [2], the problem of completing a matrix with columns from *multiple subspaces* remains a widely open problem. In this paper, we have seen surprisingly good performance with the ℓ^1-minimization. However, there is no proof yet whether this is the best one can do for this problem, nor is there

a clear characterization for the amount of entries needed.

Empirically, we have observed that the sparse coefficients $\boldsymbol{c}$ computed in our method are very suggestive of the membership of motion trajectories involved. This somehow suggests that the sparse coefficients can be used as a measure of *similarity* for the trajectories' membership. Hence one could potentially use graphical cut or spectral clustering methods for segmenting the trajectories. It would be interesting to find out if such an approach could lead to competitive clustering results than other similarity measures such as the local subspace affinity [31], or even better than the methods proposed in this paper.

ACKNOWLEDGMENT

This work is partially supported by grants NSF CRS-EHS-0509151, NSF CCF-TF-0514955, ONR YIP N00014-05-1-0633, NSF IIS 07-03756, NSF CAREER IIS-0447739, NSF EHS-0509101, and ONR N00014-05-10836, and by contract JHU APL-934652.

REFERENCES

[1] A. Barron, J. Rissanen, and B. Yu. The Minimum Description Length Principle in Coding and Modeling. *IEEE Transactions on Information Theory*, 44(6):2743–2760, 1998.

[2] E. Candes and B. Recht. Exact matrix completion via convex optimization. preprint, *http://www.ist.caltech.edu/∼brecht/papers/08.Candes.Recht.MatrixCompletion.pdf*, May 2008.

[3] E. Candes, M. Rudelson, R. Vershynin, and T. Tao. Error Correction via Linear Programming. *Proceedings of the IEEE Symposium on Foundations of Computer Science*, pages 295–308, 2005.

[4] E. Candes and T. Tao. Decoding by Linear Programming. *IEEE Transactions on Information Theory*, 2005.

[5] J. Costeira and T. Kanade. A multibody factorization method for independently moving objects. *International Journal of Computer Vision*, 29(3):159–179, 1998.

[6] M. Datar, N. Immorlica, P. Indyk, and V. Mirrokni. Locality-sensitive hashing scheme based of p-stable distributions. *Proceedings of the ACM Symposium on Computational Geometry*, 2004.

[7] F. De la Torre and M. J. Black. Robust principal component analysis for computer vision. In *Proceedings of the International Conference on Computer Vision*, pages 362–369, 2001.

[8] D. L. Donoho. For most large underdetermined systems of linear equations the minimal ℓ^1-norm solution is also the sparsest solution. preprint, *http://www-stat.stanford.edu/∼donoho/reports.html*, September 2004.

[9] D. L. Donoho and J. Tanner. Counting faces of randomly projected polytopes when the projection radically lowers dimension. preprint, *http://www.math.utah.edu/∼tanner/*, 2007.

[10] Z. Fan, J. Zhou, and Y. Wu. Multibody Grouping by Inference of Multiple Subspaces from High Dimensional Data Using Oriented-Frames. *IEEE Transactions on Pattern Analysis and Machine Intelligence*, 28(1):90–105, Jan 2006.

[11] M. Fazel, H. Hindi, and S. Boyd. Log-det heuristic for matrix rank minimization with applications to Hankel and Euclidean distance matrices. In *Proceedings of the American Control Conference*, pages 2156–2162, Jun 2003.

[12] C. Gear. Multibody grouping from motion images. *International Journal of Computer Vision*, 29(2):133–150, 1998.

[13] M. Grant and S. Boyd. CVX: MATLAB software for disciplined convex programming [web page and software]. *http://www.stanford.edu/∼boyd/cvx/*, November 2007.

[14] A. Gruber and Y. Weiss. Multibody factorization with uncertainty and missing data using the EM algorithm. In *Proceedings of the IEEE Conference on Computer Vision and Pattern Recognition*, volume 1, pages 769–775, 2004.

[15] R. Hartley and F. Schaffalitzky. PowerFactorization: an approach to affine reconstruction with missing and uncertain data. *Australia-Japan Advanced Workshop on Computer Vision*, 2003.

[16] N. Ichimura. Motion segmentation based on factorization and discriminant criterion. In *Proceedings of the International Conference on Computer Vision*, pages 600–605, 1999.

[17] K. Kanatani. Motion segmentation by subspace separation and model selection. In *Proceedings of the International Conference on Computer Vision*, volume 2, pages 586–591, 2001.

[18] K. Kanatani and Y. Sugaya. Multi-stage optimization for multi-body motion segmentation. *Australia-Japan Advanced Workshop on Computer Vision*, 2003.

[19] Q. Ke and T. Kanade. Robust ℓ^1-norm factorization in the presence of outliers and missing data by alternative convex programming. In *Proceedings of the IEEE Conference on Computer Vision and Pattern Recognition*, pages 739–746, 2005.

[20] Y. Ma, H. Derksen, W. Hong, and J. Wright. Segmentation of multivariate mixed data via lossy coding and compression. *IEEE Transactions on Pattern Analysis and Machine Intelligence*, 29(9):1546–1562, September 2007.

[21] B. Recht, M. Fazel, and P. A. Parillo. Guaranteed minimum-rank solutions of linear matrix equations via nuclear norm minimization. preprint, *http://www.ist.caltech.edu/∼brecht/papers/07.rfp.lowrank.pdf*, 2007.

[22] K. Schindler, D. Suter, and H. Wang. A model-selection framework for multibody structure-and-motion of image sequences. *International Journal of Computer Vision*, 2008.

[23] P. Torr. Geometric motion segmentation and model selection. *Phil. Trans. Royal Society of London*, pages 1321–1340, 1998.

[24] R. Tron and R. Vidal. A benchmark for the comparison of 3-D motion segmentation algorithms. In *Proceedings of the IEEE Conference on Computer Vision and Pattern Recognition*, pages 1–8, 2007.

[25] L. Vandenberghe and S. Boyd. Semidefinite programming. *SIAM Review*, 38(1):49–95, Mar 1996.

[26] R. Vidal, Y. Ma, and S. Sastry. Generalized Principal Component Analysis (GPCA). *IEEE Transactions on Pattern Analysis and Machine Intelligence*, 27(12):1–15, 2005.

[27] R. Vidal, R. Tron, and R. Hartley. Multiframe motion segmentation with missing data using PowerFactorization and GPCA. *International Journal of Computer Vision*, 2007.

[28] J. Wright and Y. Ma. Dense Error Correction via ℓ^1 Minimization. *submitted to IEEE Transactions on Information Theory*, 2008.

[29] J. Wright, Y. Ma, Y. Tao, Z. Lin, and H.-Y. Shum. Classification via minimum incremental coding length (MICL). *submitted to SIAM Journal of Imaging Sciences*, 2008.

[30] J. Wright, A. Y. Yang, A. Ganesh, Y. Ma, and S. S. Sastry. Robust Face Recognition via Sparse Representation. *to appear in IEEE Transactions on Pattern Analysis and Machine Intelligence*, 2008.

[31] J. Yan and M. Pollefeys. A general framework for motion segmentation: independent, articulated, rigid, non-rigid, degenerate and non-degenerate. In *Proceedings of the European Conference on Computer Vision*, pages 94–106, 2006.

[32] A. Y. Yang, S. Rao, and Y. Ma. Robust statistical estimation and segmentation of multiple subspaces. In *CVPR Workshop on 25 Years of RANSAC*, 2006.

[33] L. Zelnik-Manor and M. Irani. Degeneracies, dependencies and their implications in multi-body and multi-sequence factorization. In *Proceedings of the IEEE Conference on Computer Vision and Pattern Recognition*, volume 2, pages 287–293, 2003.

Shankar Rao received his bachelor's degree in electrical engineering and computer science from the University of California, Berkeley in 2001. He received his MS degree in electrical and computer engineering in 2004, and another MS degree in Applied Mathematics in 2006, both from the University of Illinois at Urbana-Champaign. He is currently a PhD candidate in the Department of Electrical and Computer Engineering at the University of Illinois. His research interests include lossy coding-based clustering, robust subspace segmentation, manifold learning, and motion/video segmentation.

Roberto Tron received his BSc degree in 2004 and MSc degree (highest honors) in 2007 both in Telecommunication Engineering from the Politecnico di Torino. He also received a Diplome d'Engenieur from the Eurecom Institute and a DEA degree from the Université de Nice Sophia-Antipolis in 2006. He is currently a PhD student in the Department of Electrical and Computer Engineering at the Johns Hopkins University. His research interests include motion segmentation and distributed algorithms on camera sensor networks.

René Vidal received the BSc degree (highest honors) in Electrical Engineering from the Universidad Católica de Chile in 1997 and the MSc and PhD degrees in Electrical Engineering and Computer Sciences from the University of California at Berkeley in 2000 and 2003, respectively. In 2004 he joined The Johns Hopkins University as an Assistant Professor in the Department of Biomedical Engineering and the Center for Imaging Science. He was co-editor (with Anders Heyden and Yi Ma) of the book "Dynamical Vision" and has co-authored more than 100 articles in biomedical imaging, computer vision, machine learning, hybrid systems, robotics, and vision-based control. Dr. Vidal is Associate Editor of the Journal of Mathematical Imaging and Vision, and member of the Program Committee of all major computer vision conferences. Dr. Vidal is recipient of the 2005 NSF CAREER Award, the 2004 Best Paper Award Honorable Mention at the European Conference on Computer Vision, the 2004 Sakrison Memorial Prize, the 2003 Eli Jury Award, and the 1997 Award of the School of Engineering of the Universidad Católica de Chile to the best graduating student of the school. He is a member of the IEEE.

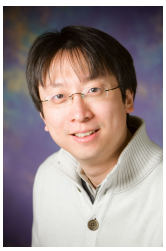

Yi Ma (SM'06) received his two Bachelors' degrees in Automation and Applied Mathematics from Tsinghua University, Beijing, China in 1995. He received an M.S. degree in Electrical Engineering and Computer Science (EECS) in 1997, an M.A. degree in Mathematics in 2000, and a PhD degree in EECS in 2000 all from UC Berkeley. Since 2000, he has been on the faculty of the Electrical & Computer Engineering Department of the University of Illinois at Urbana-Champaign, where he now holds the rank of associate professor. Currently, he is also the research manager for the Visual Computing Group of Microsoft Research Asia in Beijing. His main research areas are in systems theory and computer vision. Yi Ma was the recipient of the David Marr Best Paper Prize at the International Conference on Computer Vision in 1999 and Honorable Mention for the Longuet-Higgins Best Paper Award at the European Conference on Computer Vision in 2004. He received the CAREER Award from the National Science Foundation in 2004 and the Young Investigator Program Award from the Office of Naval Research in 2005. He is an associate editor for the IEEE Transactions on Pattern Analysis and Machine Intelligence. He is a senior member of IEEE and a member of ACM.

Summary of Improvements upon our CVPR '08 paper

* We improved the computational complexity of our Agglomerative Lossy Compression algorithm by applying the rank-1 Cholesky update. In our experiments, this modification results in a two to four times speedup of our algorithm.
* We obtained four new motion sequences containing real outlying, incomplete, and corrupted trajectories. Based on these sequences, we include three new experiments evaluating the performance of our algorithm in the presence of each kind of pathological trajectory.
* In our experiments with synthetic missing data, we now compare our l1-based approach with the Power Factorization (PF) method of Hartley.
* In our experiments with real missing data, we now compare our l1-based approach with both PF and the Robust Principal Component Analysis (RPCA) method of De la Torre (previously we only compared with PF).
* In our experiments with real corrupted data, we now compare our l1-based approach with RPCA.

Motion Segmentation via Robust Subspace Separation in the Presence of Outlying, Incomplete, or Corrupted Trajectories *

Shankar R. Rao† Roberto Tron‡ René Vidal‡ Yi Ma†

†Coordinated Science Laboratory
University of Illinois at Urbana-Champaign
{srrao,yima}@uiuc.edu

‡Center for Imaging Science
Johns Hopkins University
{tron,rvidal}@cis.jhu.edu

Abstract

We examine the problem of segmenting tracked feature point trajectories of multiple moving objects in an image sequence. Using the affine camera model, this motion segmentation problem can be cast as the problem of segmenting samples drawn from a union of linear subspaces. Due to limitations of the tracker, occlusions and the presence of nonrigid objects in the scene, the obtained motion trajectories may contain grossly mistracked features, missing entries, or not correspond to any valid motion model. In this paper, we develop a robust subspace separation scheme that can deal with all of these practical issues in a unified framework. Our methods draw strong connections between lossy compression, rank minimization, and sparse representation. We test our methods extensively and compare their performance to several extant methods with experiments on the Hopkins 155 database. Our results are on par with state-of-the-art results, and in many cases exceed them. All MATLAB code and segmentation results are publicly available for peer evaluation at `http://perception.csl.uiuc.edu/coding/motion/`.

1. Introduction

A fundamental problem in computer vision is to infer structures and movements of 3D objects from a video sequence. While classical multiple-view geometry typically deals with the situation where the scene is static, recently there has been growing interest in the analysis of dynamic scenes. Such scenes often contain multiple motions, as there could be multiple objects moving independently in a scene, in addition to camera motion. Thus an important initial step in the analysis of video sequences is the *motion segmentation* problem. That is, given a set of feature points that are tracked through a sequence of video frames, one seeks to cluster the trajectories of those points according to different motions.

In the literature, many different camera models have been proposed and studied, such as paraperspective, orthographic, affine and perspective. Among these the affine camera model is arguably the most popular, due largely to its generality and simplicity. Thus, in this paper, we assume the affine camera model, and show how to develop a robust solution to the motion segmentation problem. Before we delve into our problems of interest, we first review the basic mathematical setup.

Basic Formulation of Motion Segmentation. Suppose we are given trajectories of P tracked feature points of a rigid object $\{(x_{fp}, y_{fp})\}_{f=1\ldots F}^{p=1\ldots P}$ from F 2-D image frames of a rigidly moving camera. The affine camera model stipulates that these tracked feature points are related to their 3-D coordinates $\{(X_p, Y_p, Z_p)\}_{p=1}^{P}$ by the matrix equation:

$$\underbrace{\begin{bmatrix} x_{11} & x_{12} & \cdots & x_{1P} \\ y_{11} & y_{12} & \cdots & y_{2P} \\ \vdots & \vdots & \ddots & \vdots \\ x_{F1} & x_{F2} & \cdots & x_{FP} \\ y_{F1} & y_{F2} & \cdots & y_{FP} \end{bmatrix}}_{\mathtt{Y}\in\mathbb{R}^{2F\times P}} = \underbrace{\begin{bmatrix} A_1 \\ \vdots \\ A_F \end{bmatrix}}_{\mathtt{A}\in\mathbb{R}^{2F\times 4}} \underbrace{\begin{bmatrix} X_1 & \cdots & X_P \\ Y_1 & \cdots & Y_P \\ Z_1 & \cdots & Z_P \\ 1 & \cdots & 1 \end{bmatrix}}_{\mathtt{X}\in\mathbb{R}^{4\times P}},$$

$$\mathtt{Y} = \mathtt{A}\mathtt{X} \tag{1}$$

where $A_f = K_f \begin{bmatrix} 1 & 0 & 0 & 0 \\ 0 & 1 & 0 & 0 \\ 0 & 0 & 0 & 1 \end{bmatrix} \begin{bmatrix} R_f & \boldsymbol{t}_f \\ \mathbf{0}^T & 1 \end{bmatrix} \in \mathbb{R}^{2\times 4}$ is the *affine motion matrix* at frame f. The affine motion matrix is parameterized by the camera calibration matrix $K_f \in \mathbb{R}^{2\times 3}$ and the relative orientation of the rigid object w.r.t. the camera $(R_f, \boldsymbol{t}_f) \in SE(3)$. From this formulation we see that

$$\operatorname{rank}(\mathtt{Y}) = \operatorname{rank}(\mathtt{A}\mathtt{X}) \leq \min(\operatorname{rank}(\mathtt{A}), \operatorname{rank}(\mathtt{X})) \leq 4. \tag{2}$$

Thus the affine camera model postulates that trajectories of feature points from a single rigid motion will all lie in a linear subspace of $\mathbb{R}^{2F}$ of dimension at most four.

A dynamic scene can contain multiple moving objects, in which case the affine camera model for a single rigid motion cannot be directly applied. Now let us assume that the given P trajectories correspond to N moving objects. In this case, the set of all trajectories will lie in a *union of N linear subspaces* in $\mathbb{R}^{2F}$, but we do not know which trajectory belongs to which subspace. Thus, the problem of assigning each trajectory to its corresponding motion reduces to the problem

*This work was partially supported by grants NSF EHS-0509151, NSF CCF-0514955, ONR YIP N00014-05-1-0633, NSF IIS-0703756, NSF CAREER 0447739, NSF EHS-0509101, ONR N00014-05-1083 and WSE/APL Contract: Information Fusion & Localization in Distributed Sensor Systems.

of segmenting data drawn from multiple subspaces, which we refer to as *subspace separation*.

Problem 1 (Motion Segmentation via Subspace Separation). *Given a set of trajectories of P feature points $\mathtt{Y} = [\boldsymbol{y}_1 \dots \boldsymbol{y}_P] \in \mathbb{R}^{2F \times P}$ from N rigidly moving objects in a dynamic scene, find a permutation Γ of the columns of the data matrix $\mathtt{Y}$:*

$$\mathtt{Y} = [\mathtt{Y}_1 \dots \mathtt{Y}_N]\Gamma^{-1}, \tag{3}$$

such that the columns of each submatrix $\mathtt{Y}_n$, $n = 1, \dots, N$, are trajectories of a single motion.

Related Work on Motion Segmentation. In the literature, there are many approaches to motion segmentation, that can roughly be grouped into three categories: factorization-based, algebraic, and statistical.

Many early attempts at motion segmentation attempt to directly factor $\mathtt{Y}$ according to (3) [1, 7, 11, 12]. To make such approaches tractable, the motions must be independent of one another, *i.e.* the pairwise intersection of the motion subspaces must be the zero vector. However, for most dynamic scenes with a moving camera or containing articulated objects, the motions are at least partially dependent on each other. This has motivated the development of algorithms designed to deal with dependent motions.

Algebraic methods, such as Generalized Principal Component Analysis (GPCA) [19], are generic subspace separation algorithms that do not place any restriction on the relative orientations of the motion subspaces. However, when a linear solution is used, the complexity of algebraic methods grows *exponentially* with respect to both the dimension of the ambient space and the number of motions in the scene, and so algebraic methods are not scalable in practice.

The statistical methods come in many flavors. Many formulate motion segmentation as a statistical clustering problem that is tackled with Expectation-Maximization (EM) or variations of it [17, 13, 9]. As such, they are iterative methods that require good initialization, and can potentially get stuck in suboptimal local minima. Other statistical methods use local information around each trajectory to create a pairwise similarity matrix that can then be segmented using *spectral clustering* techniques [24, 22, 5].

Robustness Issue and Our Approach. Many of the above approaches assume that all trajectories are good, with perhaps a moderate amount of noise. However, real motion data acquired by a tracker can be much more complicated:

1. A trajectory may correspond to certain nonrigid or random motions that do not obey the affine camera model (an *outlying trajectory*).
2. Some of the features may be missing in some frames, causing a trajectory to have some missing entries (an *incomplete trajectory*).
3. Even worse, some feature points may be mistracked (with the tracker unaware), causing a trajectory to have some entries with gross errors (a *corrupted trajectory*).

While some of the methods can be modified to be robust to *one* of such problems [9, 5, 23, 22, 20], to our knowledge there is no motion segmentation algorithm that can elegantly deal with all of these problems in a unified fashion.

In this paper, we propose a new motion segmentation scheme that draws heavily from the principles of *data compression* and *sparse representation*. We show that the new algorithm naturally handles outlying trajectories, and can be designed to repair incomplete or corrupted trajectories.[1] Our methods use the affine camera model assumption, so we do not make any comparisons with perspective camera-based methods[2]. As most extant methods for motion segmentation assume that the number of motions is known, for fair comparison, we also assume the group count is given.

2. Robust Subspace Separation

In this section, we describe the subspace separation method that we use for motion segmentation and show that by properly exploiting the low rank subspace structure in the data, our method can be made robust to the three kinds of pathological trajectories discussed earlier.

To a large extent, the goal of subspace separation is to find a partition of the data matrix $\mathtt{Y}$ into submatrices $\{\mathtt{Y}_n\}_{n=1}^N$ such that each $\mathtt{Y}_n$ is maximally rank deficient. *Matrix rank minimization* (MRM) is itself a very challenging problem. The rank function is neither smooth nor convex, and so finding a matrix $\mathtt{M}$ that is maximally rank deficient among a convex set of matrices is known to be NP-Hard. Also, the rank function is highly unstable in the presence of noise. For a positive semidefinite matrix $\mathtt{M} \in \mathbb{R}^{D \times D}$, one can deal with both instability and computational intractability by minimizing the following smooth surrogate for $\text{rank}(\mathtt{M})$:

$$J(\mathtt{M}, \delta) \doteq \log_2 \det\left(\delta \mathtt{I} + \mathtt{M}\right), \tag{4}$$

where $\delta > 0$ is a small regularization parameter [6].

As we are not minimizing $\text{rank}(\mathtt{Y}_n)$ over a convex set, subspace separation is not technically an instance of MRM. However, after a slight modification to (4), we can see a connection between MRM and the principle of *lossy minimum description length* (LMDL). Given data $\mathtt{Y}_n \in \mathbb{R}^{D \times P_n}$ drawn from a linear subspace, the number of bits needed to code the data $\mathtt{Y}_n$ up to distortion ε^2 [15] [3] is given by

[1] We make a distinction between incomplete and corrupted trajectories: for incomplete trajectories, we know in which frames the features are missing; for corrupted ones, we do not have that knowledge.

[2] Please refer to [16] for work on robust motion segmentation with a perspective camera model.

[3] It can be shown that as $\varepsilon \to 0$, (5) converges to the optimal coding length for a Gaussian source, and is also an upper bound for the coding length of subspace-like data.

$$L(\mathtt{Y}_n,\varepsilon) \doteq \frac{D+P_n}{2}\left[J\left(\frac{1}{P_n}\mathtt{Y}_n\mathtt{Y}_n^T,\frac{\varepsilon^2}{D}\right)-\log_2\det\left(\frac{\varepsilon^2}{D}\mathtt{I}\right)\right]$$
$$= \frac{D+P_n}{2}\log_2\det\left(\mathtt{I}+\frac{D}{P_n\varepsilon^2}\mathtt{Y}_n\mathtt{Y}_n^T\right). \quad (5)$$

$L(\mathtt{Y}_n,\varepsilon)$ is still a smooth surrogate for rank$(\mathtt{Y}_n)$, as it is obtained by subtracting a constant term from $J(\mathtt{M},\delta)$, with $\mathtt{M}=\frac{1}{P_n}\mathtt{Y}_n\mathtt{Y}_n^T$ and $\delta=\frac{\varepsilon^2}{D}$, and scaling by a constant factor.

Now suppose the data matrix $\mathtt{Y}\in\mathbb{R}^{D\times P}$, can be partitioned into disjoint subsets $\mathtt{Y}=[\mathtt{Y}_1\ldots\mathtt{Y}_N]$ of corresponding sizes $P_1+\cdots+P_N=P$. If we encode each subset separately, the total number of bits required is

$$L^s(\{\mathtt{Y}_1,\ldots,\mathtt{Y}_N\},\varepsilon)\doteq\sum_{n=1}^{N}L(\mathtt{Y}_n,\varepsilon)-P_n\log_2\frac{P_n}{P}. \quad (6)$$

The second term in this equation counts the number of bits needed to represent the membership of the P vectors in the N subsets (*i.e.* by Huffman coding). In [15], Ma *et al.* posit that the optimal segmentation of the data minimizes the number of bits needed to encode the segmented data up to distortion ε^2.

Finding a global minimum of (6) is a combinatorial problem. Nevertheless, an agglomerative algorithm, proposed in [15], has been shown to be very effective for minimizing (6). It initially treats each sample as its own group, iteratively merging pairs of groups so that the resulting coding length is maximally reduced at each iteration. The algorithm terminates when it can no longer reduce the coding length. We refer to their algorithm as *Agglomerative Lossy Compression* (ALC). See [15] for more details.

2.1. Outlying Trajectories

Dynamic scenes often contain trajectories that do not correspond to any of the motion models in the scene. Such outlying trajectories can arise from motions not well described by the affine camera model, such as the motion of non-rigid objects. These kinds of trajectories have been referred to as "sample outliers" by [2], suggesting that no subset of the trajectory corresponds to any affine motion model. Fortunately, ALC deals with these outliers in an elegant fashion. In [15], it was observed that in low dimensions (≤ 3), all outliers tend to cluster into a single group. This is because in low dimensions it is very unlikely that outliers live in a lower-dimensional subspace. Hence it is more efficient to code them together with respect to a single basis for the ambient space. Such a group can be easily detected, because the number of bits per vector in that group is very large relative to other groups. However, in higher-dimensional spaces, such as in our motion segmentation problem, outliers are more sparsely distributed. Hence, it is more efficient to code them by representing each outlier as a separate group. Such small groups are also easily detectable.

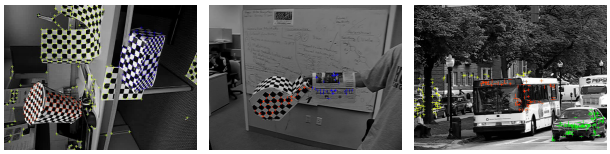

Figure 1. The motions sequences "1R2RC" (left), "arm" (center), and "cars10"(right) from the Hopkins155 database [18].

Experiments. For all of the experiments in Section 2, we choose three representative sequences from the Hopkins155 motion segmentation database [18] for testing: "1R2RC" (checkerboard), "arm" (articulation), and "cars10" (traffic) (see Figure 1). We compare the robustness to outliers of ALC and Local Subspace Affinity (LSA) [22], a spectral clustering-based motion segmentation algorithm that is reasonably robust to outliers. We add between 0% and 25% outlying trajectories to the dataset of a given motion sequence. Outlying trajectories were generated by choosing a random initial point in the first frame, and then performing a random walk through the following frames. Each increment is generated by taking the difference between the coordinates of a randomly chosen point in two randomly chosen consecutive frames. In this way the outlying trajectories will qualitatively have the same statistical properties as the other trajectories, but will not obey to any particular motion model. We then input these outlier-ridden datasets into LSA and ALC, respectively, and compute the misclassification rate and outlier detection rate for both algorithms.[4] For each experiment we run 100 trials with different randomly generated outlying trajectories. Table 1 shows the average misclassification rates and outlier detection rates for each experiment. As the results show, ALC can easily detect outliers without hindering motion segmentation, whereas for LSA, the outliers tend to interfere with the classification of valid trajectories.

Table 1. Top: Misclassification rates for LSA and ALC as a function of the outlier percentage (from 0% to 25%) for three motion sequences. Bottom: Outlier Detection rates for LSA and ALC as a function of the outlier percentage for three motion sequences.

	1R2RC [%]		arm [%]		cars10 [%]	
[%]	LSA	ALC	LSA	ALC	LSA	ALC
0	2.40	1.09	22.08	0.00	16.84	1.34
7	6.91	1.29	24.17	0.13	31.97	0.40
15	3.09	1.31	15.38	0.06	26.43	0.19
25	2.69	1.16	10.25	0.04	24.59	0.17

	1R2RC [%]		arm [%]		cars10 [%]	
[%]	LSA	ALC	LSA	ALC	LSA	ALC
0	98.04	100	77.9	100	86.87	100
7	94.75	99.99	92.79	100	96.82	99.70
15	98.04	99.98	91.34	100	98.84	99.81
25	98.20	99.97	95.56	100	98.76	99.83

[4] In ALC a trajectory is labeled an outlier if it belongs to a group with less than five samples. In our implementation of LSA, a trajectory is labeled as an outlier if its distance from the nearest motion subspace is greater than a predetermined threshold.

2.2. Incomplete Trajectories

In practice, due to occlusions or limitations of the tracker, some features may be missing in some frames. This can lead to incomplete trajectories. However by harnessing the low rank subspace structure of the data set, it is possible to complete these trajectories prior to subspace separation.

The key observation is that samples drawn from a low-dimensional linear subspace are self-expressive, meaning that a sample can be expressed in terms of a few other complete samples from the same linear subspace. More precisely, if the given incomplete sample is $\boldsymbol{y} \in \mathbb{R}^D$ and $\mathtt{Y} \in \mathbb{R}^{D \times P}$ is the matrix whose columns are all the complete samples in the data set, then there exists a coefficient vector $\boldsymbol{c} \in \mathbb{R}^P$ that satisfies

$$\boldsymbol{y} = \mathtt{Y}\boldsymbol{c}. \tag{7}$$

As the number of samples P is usually much greater than the dimension of the ambient space D, (7) is a highly underdetermined system of linear equations, and so, in general, $\boldsymbol{c}$ is not unique. In fact, any D vectors in the set that span $\mathbb{R}^D$ can serve as a basis for representing $\boldsymbol{y}$. However, since $\boldsymbol{y}$ lies in a low-dimensional linear subspace, it can be represented as a linear combination of only a few vectors from the same subspace. Hence, its coefficient vector should have only a few nonzero entries corresponding to vectors from the same subspace. Thus, what we seek is the *sparsest* $\boldsymbol{c}$:

$$\boldsymbol{c}^* = \underset{\boldsymbol{c}}{\operatorname{argmin}} \|\boldsymbol{c}\|_0 \ \text{ subject to } \ \boldsymbol{y} = \mathtt{Y}\boldsymbol{c}, \tag{8}$$

where $\|\cdot\|_0$ is the "ℓ^0 norm", equal to the number of nonzero entries in the vector. The sparsest coefficient vector $\boldsymbol{c}^*$ is unique when $\|\boldsymbol{c}^*\|_0 < D/2$. In the general case, ℓ^0 minimization, like MRM, is known to be NP-Hard [5]. Fortunately, due to the findings of Donoho *et al*. [3], it is known that if $\boldsymbol{c}^*$ is sufficently sparse (*i.e*. $\|\boldsymbol{c}^*\|_0 \lesssim \lfloor \frac{D+1}{3} \rfloor$), then the ℓ^0 minimization in (8) is equivalent to the following ℓ^1 minimization:

$$\boldsymbol{c}^* = \underset{\boldsymbol{c}}{\operatorname{argmin}} \|\boldsymbol{c}\|_1 \ \text{ subject to } \ \boldsymbol{y} = \mathtt{Y}\boldsymbol{c}, \tag{9}$$

which is essentially a linear program.

We apply these results to the problem of dealing with incomplete data. We assume that we have a set of samples $\mathtt{Y} \in \mathbb{R}^{D \times P}$ on the N subspaces with *no* missing entries, and we use $\mathtt{Y}$ to complete each sample with missing entries *individually*. Suppose $\boldsymbol{y} \in \mathbb{R}^D$ is a sample with missing entries $\{y_i\}_{i \in I}, I \subset \{1, \ldots, D\}$. Let $\hat{\boldsymbol{y}} \in \mathbb{R}^{D-|I|}$ and $\hat{\mathtt{Y}} \in \mathbb{R}^{(D-|I|) \times P}$ be $\boldsymbol{y}$ and $\mathtt{Y}$ with the rows indexed by I removed, respectively. By removing these rows, we are essentially projecting the data onto the $(D-|I|)$-dimensional subspace orthogonal to span$(\{\boldsymbol{e}_i : i \in I\})$.[6] With probability one, an arbitrary d-dimensional projection preserves the structural relationships between the subspaces, as long as the dimension of each subspace is strictly less than d. Thus if we solve the linear program:[7]

$$\boldsymbol{c}^* = \underset{\boldsymbol{c}}{\operatorname{argmin}} \|\boldsymbol{c}\|_1 \ \text{ subject to } \ \hat{\boldsymbol{y}} = \hat{\mathtt{Y}}\boldsymbol{c}, \tag{10}$$

then the completed vector $\boldsymbol{y}^*$ can be recovered as

$$\boldsymbol{y}^* = \mathtt{Y}\boldsymbol{c}^*. \tag{11}$$

In the literature there are many methods for filling in missing entries of a low rank matrix [10, 9, 14]. It is important to note that low rank matrix completion is quite different from our task here. For a matrix with low column rank, the problem of completing missing data is *overdetermined*. Thus algorithms like Power Factorization (PF) [20] essentially solve for the missing entries in a least-squares (minimum ℓ^2 norm) sense to preserve the low rank of the matrix. However, data drawn from a union of subspaces will, in general, be full rank – the matrix $\hat{\mathtt{Y}}$ is often over-complete. As such, the problem becomes instead *underdetermined* so there is no unique solution for the values of the missing entries. Our method then chooses the unique solution with the minimum ℓ^1 (and hence minimum ℓ^0) norm. The vector with missing entries is represented by the fewest possible complete vectors, which will in general be from only one of the subspaces. On the other hand, the least-squares (ℓ^2) solution found with Power Factorization is typically not sparse [3]. Table 2 compares our method to Power Factorization suggested in [20] for motion segmentation with missing data. As we see, in the case when the problem is underdetermined, the ℓ^1 solution indeed gives a much more accurate completion for the missing entries.

Table 2. Average errors over 100 trials in pixels per missing entry for Power Factorization (with rank 5) [20] and our ℓ^1-based feature completion method on the same three motion sequences used in the previous experiment (Figure 1). For each trial, 10% of the entries of the data matrix are removed and we use 75% of the complete trajectories to fill in the missing entries.

1R2RC [pixel]		arm [pixel]		cars10 [pixel]	
PF	ℓ^1	PF	ℓ^1	PF	ℓ^1
0.177	0.033	8.568	0.070	0.694	0.212

Experiments. We now test the limits of our ℓ^1-based method for entry completion. In each trial, we randomly select a trajectory $\boldsymbol{y}_p$ from the dataset for a given sequence, and remove between 1 and $D-1 = 2F-1$ of its entries. We then apply (10) and (11) to recover the missing entries[8]. In order to simulate many trajectories with missing entries in the dataset, we perform 5 different experiments. In each experiment, we use a portion (from 20% to 100%) of the remaining dataset to complete $\boldsymbol{y}_p$. Figure 2 (top) shows the results for 200 trials. For each sequence, we plot

[5] In fact, when MRM is applied to a set of *diagonal* matrices, it reduces to ℓ^0 minimization.

[6] $\boldsymbol{e}_i$ is the i-th vector in the canonical basis for $\mathbb{R}^D$.

[7] As suggested in [21], one can deal with noisy data by replacing the equality constraint in (10) with $\|\hat{\boldsymbol{y}} - \hat{\mathtt{Y}}\boldsymbol{c}\|_2 \leq \epsilon$.

[8] For all of our experiments that use ℓ^1-minimization, we use the freely available CVX toolbox for MATLAB [8].

the average per-entry error of the recovered trajectory w.r.t. the ground truth versus the percentage of missing entries in each incomplete trajectory. The different colored plots are for the experiments with varying percentage of the dataset used for completion. We see that for all motion sequences, our method is able to reconstruct trajectories to within subpixel accuracy even with over 80% of the entries missing! We also see that the performance remains consistent even when the entries are completed with small subsets of the remaining data. This suggests that our method can work well even if a large number of trajectories have missing features.

2.3. Corrupted Trajectories

Corrupted entries can be present in a trajectory when the tracker unknowingly loses track of feature points.[9] Such entries contain gross errors. One could treat corrupted trajectories as outliers.[10] However, in a corrupted trajectory, a portion of the entries still correspond to a motion in the scene, hence it seems wasteful to simply discard such information.

Repairing a vector with corrupted entries is much more difficult than the entry completion problem in Section 2.2, as now both the number and location of the corrupted entries in the vector are *not known*. Once again, by taking advantage of the low rank subspace structure of the dataset, we can both detect and repair vectors with corrupted entries *prior* to subspace separation. Our approach is similar to one proposed in [21] for robust face recognition.

A corrupted vector $\hat{\boldsymbol{y}}$ can be modeled as

$$\hat{\boldsymbol{y}} = \boldsymbol{y} + \boldsymbol{e}, \tag{12}$$

where $\boldsymbol{y}$ is the uncorrupted vector, and $\boldsymbol{e} \in \mathbb{R}^D$ is a vector that contains all of the gross errors. We assume that there are only a few gross errors, so $\boldsymbol{e}$ will only have a few nonzero entries, and thus be sparse[11]. As long as there are enough uncorrupted vectors in the dataset, we can express $\boldsymbol{y}$ as a linear combination of the other vectors in the dataset as in Section 2.2. If $\mathtt{Y} \in \mathbb{R}^{P \times D}$ is a matrix whose columns are the other vectors in the dataset, and $\mathtt{I} \in \mathbb{R}^{D \times D}$ is an identity matrix, then (12) becomes

$$\hat{\boldsymbol{y}} = \mathtt{Y}\boldsymbol{c} + \boldsymbol{e} = \begin{bmatrix} \mathtt{Y} & \mathtt{I} \end{bmatrix} \begin{bmatrix} \boldsymbol{c} \\ \boldsymbol{e} \end{bmatrix} \doteq \mathtt{B}\boldsymbol{w}. \tag{13}$$

We would like both the coefficient vector $\boldsymbol{c}$ and the error vector $\boldsymbol{e}$ to be sparse[12]. If the true $\boldsymbol{c}$ and $\boldsymbol{e}$ are sufficiently sparse, we can simultaneously find the sparsest $\boldsymbol{c}$ and $\boldsymbol{e}$ by solving the linear program:[13]

$$\boldsymbol{w}^* = \underset{\boldsymbol{w}}{\operatorname{argmin}} \|\boldsymbol{w}\|_1 \quad \text{subject to} \quad \hat{\boldsymbol{y}} = \mathtt{B}\boldsymbol{w}. \tag{14}$$

Once $\boldsymbol{w}^*$ is computed, we decompose it into $\boldsymbol{w}^* = \begin{bmatrix} \boldsymbol{c}^* & \boldsymbol{e}^* \end{bmatrix}^T$, where $\boldsymbol{c}^* \in \mathbb{R}^P$ is the recovered coefficient vector and $\boldsymbol{e}^* \in \mathbb{R}^D$ is the recovered error vector. The repaired vector $\boldsymbol{y}^*$ is simply

$$\boldsymbol{y}^* = \mathtt{Y}\boldsymbol{c}^*. \tag{15}$$

The error vector $\boldsymbol{e}^*$ also provides useful information. The nonzero entries of $\boldsymbol{e}^*$ are precisely the gross errors in $\hat{\boldsymbol{y}}$.

Experiments. We now test the limits of our ℓ^1-based method for repairing corrupted trajectories. For each trial in the experiments, we randomly select a trajectory $\boldsymbol{y}_p$ from the given dataset, and randomly *select and corrupt* between 1 and $D - 1 = 2F - 1$ entries in the vector. To corrupt the selected entries, we replace them with random values drawn from a uniform distribution. We then apply (14) and (15) to both detect the locations of corrupted entries, as well as repair them. In each experiment we run 200 trials and average the errors. We perform five experiments of this type, each with a portion (from 0% to 80%) of the remaining dataset $\mathtt{Y}$ being corrupted in the same way as $\boldsymbol{y}_p$. The results of these experiments are shown in Figure 2 (bottom). For each sequence, we plot the the average per-entry error of the repaired vector w.r.t. the ground truth versus the percentage of corrupted entries in each vector. The different colors represent experiments with varying portions of corrupted $\mathtt{Y}$. As Figure 2 (bottom) shows, this method is able to reconstruct vectors to within subpixel accuracy even with roughly 1/3 of the entries corrupted. This is in line with the bound $\|\boldsymbol{c}^*\|_0 < \lfloor \frac{D+1}{3} \rfloor$ given by [3]. We also see that the performance remains consistent even if 80% of the entire dataset is corrupted!

3. Large Scale Experiments

In this section, we perform experiments on the entire Hopkins155 database. We first discuss what modifications are needed to tailor ALC to the motion segmentation problem. We then compare our performance on the entire database versus some other motion segmentation algorithms. Finally, we do experiments on a set of motion sequences with real incomplete or corrupted trajectories.

3.1. Applying ALC to Motion Segmentation

ALC requires only a single parameter ε, the variance of the noise. However, the performance is also affected by the dimension that the original data is projected onto. Here we describe some methods for choosing these parameters.

Choosing ε. In principle, ε could be determined in some heuristic fashion from the statistics of the data. However,

[9] These kind of trajectories are called "intra-sample outliers" in [2].

[10] Indeed, if a dataset with some corrupted trajectories is input to ALC, the algorithm will classify those trajectories as outliers, as the gross errors will greatly increase the coding length of their ground-truth motion group.

[11] We realize that, in practice, trajectories may be corrupted by a large number of gross errors. However, it is unlikely that *any* method can repair such trajectories, and so it is best to treat them as outliers.

[12] The columns of $\mathtt{Y}$ should be scaled to have unit ℓ^2 norm to ensure that no vector is preferred in the sparse representation of $\boldsymbol{w}$.

[13] The presence of the identity submatrix $\mathtt{I}$ in $\mathtt{B}$ already renders the linear program stable to moderate noise.

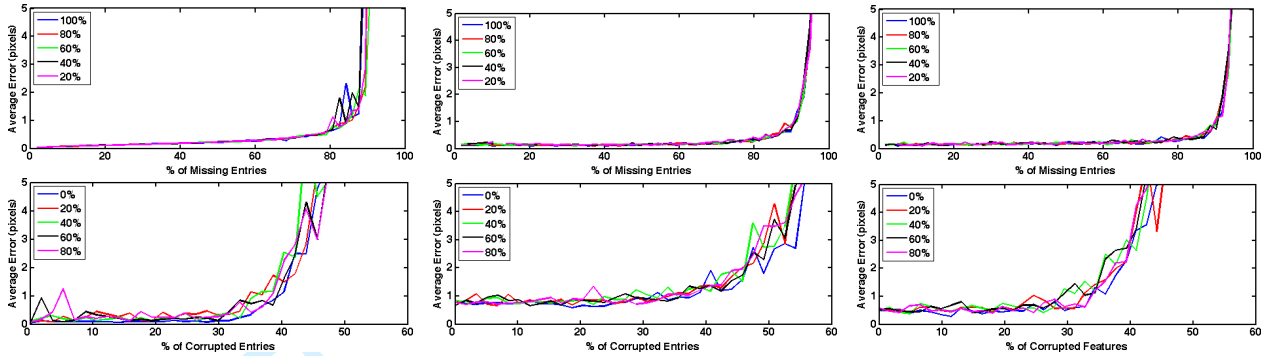

Figure 2. Errors of recovered trajectories for the sequences: "1R2RC" (left), "arm" (center), and "cars10" (right). Top: Results for our ℓ^1-based trajectory completion. The different colored plots are for experiments with varying percentage of the dataset used for completion. Bottom: Results for our ℓ^1-based detection and repair of corrupted trajectories. The different colors represent experiments with varying percentage of corrupted trajectories in the dataset.

most extant motion segmentation algorithms require the number of motions as a parameter. Thus, in order to make a fair comparison with other methods, we assume that the number of motions is given, and use it to determine ε.

Figure 3 shows an example sequence from the database. We run ALC on this sequence for several choices of ε. On the right we plot the misclassification rate and estimated group count as a function of ε. We see that the correct segmentation is stable over a fairly large interval. Using this observation, we developed the following voting scheme:

1. For a given motion sequence, run the algorithm multiple times over a number of choices of ε.[14]
2. Discard any ε that does not give rise to a segmentation with the correct number of groups.[15]
3. With the remaining choices of ε, find all the distinct segmentations that are produced.
4. Choose the ε that minimizes the coding length for the most segmentations, relative to the other choices of ε.

This scheme is quite simple, and by no means optimal, but as our experiments will show it works very well in practice.

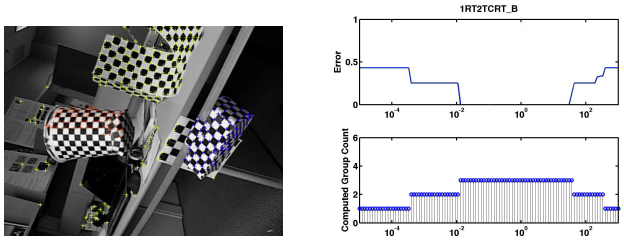

Figure 3. Left: The "1RT2TCRT_B" sequence from the Hopkins155 database. Right: The misclassification rate and estimated group count as a function of ε.

Choosing the Dimension of the Projection d. In general, Dimension Reduction improves the computational tractability of a problem. For example, for segmenting affine motions, [20] suggests projecting the trajectories onto a 5-dimensional subspace. However, for more complicated scenes (*e.g.* scenes with articulated motion), five dimensions may not be sufficient.

ALC scales roughly cubic with the dimension, so, in theory, we can leave our data in a relatively high-dimensional space. However, due to the greedy nature of the algorithm, a local minimum segmentation can be found if the samples do not adequately cover each subspace. Thus, Dimension Reduction can improve the results of ALC by increasing the density of samples within each subspace.

A balance needs to be struck between expressiveness and sample density. One choice, recently proposed in the sparse representation community [4], is the dimension d_{sp}:

$$d_{\text{sp}} = \min d \quad \text{subject to} \quad d \geq 2k \log(D/d),$$

where D is the dimension of the ambient space and k is the true low dimension of the data. It has been shown, that, asymptotically, as $D \to \infty$, this d is the smallest projection dimension such that the ℓ^1 minimization is still able to recover the correct sparse solutions. For our problem, using the affine camera model, we can assume that $k = 4$ and obtain a conservative estimate for a projection dimension d.

In our experiments, we test ALC with projection dimensions[16] $d = 5$ (as suggested in [20]), and the *sparsity-preserving* d stated above. We refer to the two versions of the algorithm as ALC_5 and ALC_{sp}, respectively.

3.2. Results on the Hopkins155 Database

The Hopkins155 database consists of 155 motion sequences categorized as checkerboard, traffic, or articulated. The motion sequences were obtained using an automatic tracker, and errors in tracking were manually corrected for each sequence. Thus in this experiment, there is no attempt to deal with incomplete or corrupted trajectories. See [18] for more details on the Hopkins155 database.

[14] Our experiments use 101 steps of ε logarithmically spaced in the interval $[10^{-5}, 10^{3}]$.

[15] If none of the choices of ε produce the right number of groups, we select the ε that minimizes the "penalized" coding length proposed in [15].

[16] We used Principal Component Analysis (PCA) as our method of Dimension Reduction.

We run ALC_5 and ALC_{sp} on the checkerboard, traffic, and articulated sequences using the voting scheme described earlier to determine ε. For each category of sequences, we compute the average and median misclassification rates, and the average computation times. We list these results in Tables 3-6 along with the reported results for Multi-Stage Learning (MSL) [13] and Local Subspace Affinity (LSA)[17] on the same database. Figure 4 gives two histograms of the misclassification rates over the sequences with two and three motions, respectively. There are several other algorithms that have been tested on the Hopkins155 database (*e.g.*, GPCA, RANSAC), but we list these two algorithms because they have the best reported misclassification rates in many categories of sequences.

As these results show, ALC performs well compared to the state-of-the-art. It has the best overall misclassification rate as well as for the checkerboard sequences. In categories where ALC is not the best, its performance is still competitive. The one notable exception is for the set of articulated sequences. In articulated sequences, it is difficult to track a lot of trajectories in each limb, but these trajectories live in a relatively high-dimensional space. Though in theory one only needs as many trajectories as the dimension of the subspace, we have observed experimentally that ALC can make suboptimal groupings when the ambient space is high-dimensional and the density of the data within a subspace is low. Finally, with regard to the projection dimension, our results indicate that, overall, ALC_{sp} performs better than ALC_5.

Table 3. Misclassification rates for sequences of two motions.

Checkerboard	MSL	LSA	ALC_5	ALC_{sp}
Average	4.46%	2.57%	2.66%	**1.55%**
Median	0.00%	0.27%	0.00%	0.29%
Traffic	MSL	LSA	ALC_5	ALC_{sp}
Average	2.23%	5.43%	2.58%	**1.59%**
Median	0.00%	1.48%	0.25%	1.17%
Articulated	MSL	LSA	ALC_5	ALC_{sp}
Average	7.23%	**4.10%**	6.90%	10.70%
Median	0.00%	1.22%	0.88%	0.95%
All Sequences	MSL	LSA	ALC_5	ALC_{sp}
Average	4.14%	3.45%	3.03%	**2.40%**
Median	0.00%	0.59%	0.00%	0.43%

3.3. Experimental Results on Robustness

We now test our robust subspace separation method on real motion sequences with incomplete or corrupted trajectories. We use the three motion sequences shown in Figure 5. These sequences are taken from [20] and are similar to the checkerboard sequences in Hopkins155. Each sequence contains three different motions and was split into three new sequences containing only trajectories from the first and second groups, first and third groups, and second and third groups, respectively. Thus, in total, we have twelve motion sequences, nine with two motions, and three with three motions. For these sequences, between 4% and 35% of the entries in the data matrix of trajectories are corrupted. These entries were manually located and labeled.

[17] For LSA we report the results for the version that projects the data onto a $4N$-dimensional space.

Table 4. Misclassification Rates for sequences of three motions.

Checkerboard	MSL	LSA	ALC_5	ALC_{sp}
Average	10.38%	5.80%	7.05%	**5.20%**
Median	4.61%	1.77%	1.02%	0.67%
Traffic	MSL	LSA	ALC_5	ALC_{sp}
Average	**1.80%**	25.07%	3.52%	7.75%
Median	0.00%	23.79%	1.15%	0.49%
Articulated	MSL	LSA	ALC_5	ALC_{sp}
Average	**2.71%**	7.25%	7.25%	21.08%
Median	2.71%	7.25%	7.25%	21.08%
All Sequences	MSL	LSA	ALC_5	ALC_{sp}
Average	8.23%	9.73%	**6.26%**	6.69%
Median	1.76%	2.33%	1.02%	0.67%

Table 5. Misclassification Rates over entire Hopkins 155 Database.

Checkerboard	MSL	LSA	ALC_5	ALC_{sp}
Average	5.94%	3.38%	3.76%	**2.47%**
Median	0.00%	0.57%	0.00%	0.31%
Traffic	MSL	LSA	ALC_5	ALC_{sp}
Average	**2.15%**	9.05%	2.76%	2.77%
Median	0.00%	1.96%	0.41%	1.10%
Articulated	MSL	LSA	ALC_5	ALC_{sp}
Average	6.53%	**4.58%**	7.58%	13.71%
Median	0.00%	1.22%	0.92%	3.46%
All Sequences	MSL	LSA	ALC_5	ALC_{sp}
Average	5.06%	4.87%	3.83%	**3.56%**
Median	0.00%	0.90%	0.27%	0.50%

Table 6. Average computation times for various algorithms.

Method	MSL	LSA	ALC_5	ALC_{sp}
Checkerboard	17h 40m	10.423s	12m 6s	24m 4s
Traffic	12h 42m	8.433s	8m 42s	17m 19s
Articulated	7h 35m	3.551s	4m 51s	10m 43s
All Sequences	19h 11m	9.474s	10m 32s	21m 3s

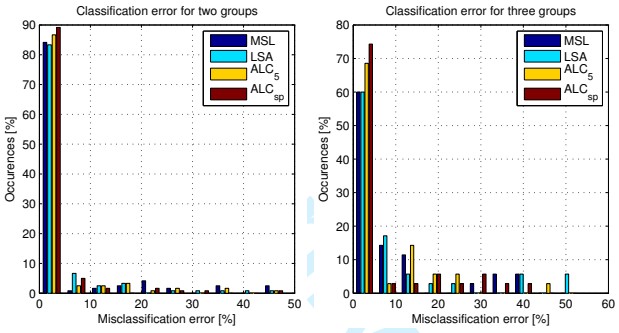

Figure 4. Misclassification rate histograms for various algorithms on the Hopkins155 database.

Incomplete Data. To see how ℓ^1-based entry completion affects the quality of segmentation, we remove the entries of

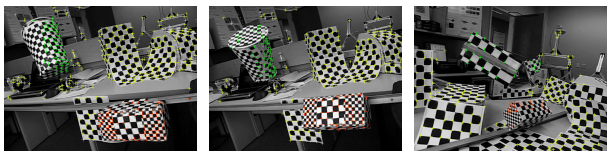

Figure 5. Example frames from three motion sequences with incomplete or corrupted trajectories. Sequences taken from [20].

trajectories that were marked as corrupted so that we may treat them as missing entries. We apply our ℓ^1-based entry completion method to this data, and input the completed data into ALC_5 and ALC_{sp}, respectively. For comparison, we also use Power Factorization to complete the data before segmentation. The misclassification rate for each sequence is listed in Table 7. The best overall results are for our ℓ^1-based method combined with ALC_{sp}. However, while Power Factorization combined with ALC_5 also performs competitively, its performance becomes much worse when combined with ALC_{sp}. These results give some empirical justification to our assertion that Power Factorization relies on the low rank of a matrix to recover missing entries.

Table 7. Misclassifications rates for Power Factorization and our ℓ^1-based approach on 12 real motion sequences with missing data.

Method	PF+ALC_5	PF+ALC_{sp}	ℓ^1+ALC_5	ℓ^1+ALC_{sp}
Average	1.89%	10.81%	3.81%	1.28%
Median	0.39%	7.85%	0.17%	1.07%

Corrupted Data. We also test our ability to repair corrupted trajectories, and observe the effects of the repair on segmentation. We simply apply our ℓ^1-based repair and detection method to the raw motion sequences, and then input the *repaired* data to ALC_5 and ALC_{sp}, respectively. The misclassification rate for each sequence is listed in Table 8. As the results show, our ℓ^1-based approach can repair corrupted trajectories to achieve reasonable segmentations.

Table 8. Misclassifications rates for our ℓ^1-based approach on 12 real motion sequences with corrupted trajectories.

Method	ℓ^1+ ALC_5	ℓ^1+ ALC_{sp}
Average	4.15%	3.02%
Median	0.21%	0.89%

4. Conclusion

In this paper we have developed a robust subspace separation method that applies Agglomerative Lossy Compression to the problem of motion segmentation. We showed that by properly exploiting the low rank nature of motion data, we can effectively deal with practical pathologies such as incomplete or corrupted trajectories. These techniques are in fact generic to subspace separation, and can conceivably be used in other application domains with little modification.

References

[1] J. Costeira and T. Kanade. A multibody factorization method for independently moving objects. *IJCV*, 29(3):159–179, 1998.

[2] F. De la Torre and M. J. Black. Robust principal component analysis for computer vision. In *ICCV*, pages 362–369, 2001.

[3] D. L. Donoho. For most large underdetermined systems of linear equations the minimal ℓ^1-norm solution is also the sparsest solution. preprint, *http://www-stat.stanford.edu/∼donoho/reports.html*, September 2004.

[4] D. L. Donoho and J. Tanner. Counting faces of randomly projected polytopes when the projection radically lowers dimension. preprint, *http://www.math.utah.edu/∼tanner/*, 2007.

[5] Z. Fan, J. Zhou, and Y. Wu. Multibody Grouping by Inference of Multiple Subspaces from High Dimensional Data Using Oriented-Frames. *IEEE TPAMI*, 28(1):90–105, Jan 2006.

[6] M. Fazel, H. Hindi, and S. Boyd. Log-det heuristic for matrix rank minimization with applications to Hankel and Euclidean distance matrices. In *Proceedings of the American Control Conference*, pages 2156–2162, Jun 2003.

[7] C. Gear. Multibody grouping from motion images. *IJCV*, 29(2):133–150, 1998.

[8] M. Grant and S. Boyd. `CVX`: MATLAB software for disciplined convex programming [web page and software]. *http://www.stanford.edu/∼boyd/cvx/*, November 2007.

[9] A. Gruber and Y. Weiss. Multibody factorization with uncertainty and missing data using the EM algorithm. In *CVPR*, volume 1, pages 769–775, 2004.

[10] R. Hartley and F. Schaffalitzky. PowerFactorization: an approach to affine reconstruction with missing and uncertain data. *Australia-Japan Advanced Workshop on Computer Vision*, 2003.

[11] N. Ichimura. Motion segmentation based on factorization and discriminant criterion. In *ICCV*, pages 600–605, 1999.

[12] K. Kanatani. Motion segmentation by subspace separation and model selection. In *ICCV*, volume 2, pages 586–591, 2001.

[13] K. Kanatani and Y. Sugaya. Multi-state optimization for multi-body motion segmentation. *Australia-Japan Advanced Workshop on Computer Vision*, 2003.

[14] Q. Ke and T. Kanade. Robust ℓ^1-norm factorization in the presence of outliers and missing data by alternative convex programming. In *CVPR*, pages 739–746, 2005.

[15] Y. Ma, H. Derksen, W. Hong, and J. Wright. Segmentation of multivariate mixed data via lossy coding and compression. *IEEE TPAMI*, 29(9):1546–1562, September 2007.

[16] K. Schindler, D. Suter, and H. Wang. A model-selection framework for multibody structure-and-motion of image sequences. *IJCV*, 2008.

[17] P. Torr. Geometric motion segmentation and model selection. *Phil. Trans. Royal Society of London*, pages 1321–1340, 1998.

[18] R. Tron and R. Vidal. A benchmark for the comparison of 3-D motion segmentation algorithms. In *CVPR*, pages 1–8, 2007.

[19] R. Vidal, Y. Ma, and S. Sastry. Generalized Principal Component Analysis (GPCA). *IEEE TPAMI*, 27(12):1–15, 2005.

[20] R. Vidal, R. Tron, and R. Hartley. Multiframe motion segmentation with missing data using PowerFactorization and GPCA. *IJCV*, 2007.

[21] J. Wright, A. Y. Yang, A. Ganesh, Y. Ma, and S. S. Sastry. Robust Face Recognition via Sparse Representation. *to appear in IEEE TPAMI*, 2008.

[22] J. Yan and M. Pollefeys. A general framework for motion segmentation: independent, articulated, rigid, non-rigid, degenerate and non-degenerate. In *ECCV*, pages 94–106, 2006.

[23] A. Y. Yang, S. Rao, and Y. Ma. Robust statistical estimation and segmentation of multiple subspaces. In *CVPR Workshop on 25 Years of RANSAC*, 2006.

[24] L. Zelnik-Manor and M. Irani. Degeneracies, dependencies and their implications in multi-body and multi-sequence factorization. In *CVPR*, volume 2, pages 287–293, 2003.